



Multichannel Detection Systems Available for Flow Diagnostics at AEDC

W. D. Williams, H. M. Powell, J. H. Jones, and R. L. McGuire
Calspan Field Services, Inc.

August 1983

Final Report for Period October 1, 1982 to September 30, 1983

Approved for public release; distribution unlimited.

**ARNOLD ENGINEERING DEVELOPMENT CENTER
ARNOLD AIR FORCE STATION, TENNESSEE
AIR FORCE SYSTEMS COMMAND
UNITED STATES AIR FORCE**

NOTICES

When U. S. Government drawings, specifications, or other data are used for any purpose other than a definitely related Government procurement operation, the Government thereby incurs no responsibility nor any obligation whatsoever, and the fact that the government may have formulated, furnished, or in any way supplied the said drawings, specifications, or other data, is not to be regarded by implication or otherwise, or in any manner licensing the holder or any other person or corporation, or conveying any rights or permission to manufacture, use, or sell any patented invention that may in any way be related thereto.

Qualified users may obtain copies of this report from the Defense Technical Information Center.

References to named commercial products in this report are not to be considered in any sense as an endorsement of the product by the United States Air Force or the Government.

This report has been reviewed by the Office of Public Affairs (PA) and is releasable to the National Technical Information Service (NTIS). At NTIS, it will be available to the general public, including foreign nations.

APPROVAL STATEMENT

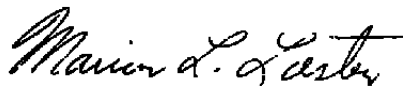
This report has been reviewed and approved.



MARSHALL K. KINGERY
Directorate of Technology
Deputy for Operations

Approved for publication:

FOR THE COMMANDER



MARION L. LASTER
Director of Technology
Deputy for Operations

UNCLASSIFIED

SECURITY CLASSIFICATION OF THIS PAGE (When Data Entered)

REPORT DOCUMENTATION PAGE		READ INSTRUCTIONS BEFORE COMPLETING FORM
1 REPORT NUMBER AEDC-TR-83-28	2 GOVT ACCESSION NO.	3 RECIPIENT'S CATALOG NUMBER
4. TITLE (and Subtitle) MULTICHANNEL DETECTION SYSTEMS AVAILABLE FOR FLOW DIAGNOSTICS AT AEDC		5 TYPE OF REPORT & PERIOD COVERED Final Report, October 1, 1982 - September 30, 1983
		6 PERFORMING ORG. REPORT NUMBER
7 AUTHOR(s) W. D. Williams, H. M. Powell, J. H. Jones, and R. L. McGuire, Calspan Field Services, Inc./AEDC Division		8. CONTRACT OR GRANT NUMBER(s)
9 PERFORMING ORGANIZATION NAME AND ADDRESS Arnold Engineering Development Center/DOT Air Force Systems Command Arnold Air Force Station, TN 37389		10 PROGRAM ELEMENT, PROJECT, TASK AREA & WORK UNIT NUMBERS Program Element 65807F
11. CONTROLLING OFFICE NAME AND ADDRESS Arnold Engineering Development Center/DOS Air Force Systems Command Arnold Air Force Station, TN 37389		12. REPORT DATE August 1983
		13. NUMBER OF PAGES 43
14 MONITORING AGENCY NAME & ADDRESS (if different from Controlling Office)		15. SECURITY CLASS. (of this report) UNCLASSIFIED
		15a. DECLASSIFICATION/DOWNGRADING SCHEDULE N/A
16. DISTRIBUTION STATEMENT (of this Report) Approved for public release; distribution unlimited.		
17. DISTRIBUTION STATEMENT (of the abstract entered in Block 20, if different from Report)		
18. SUPPLEMENTARY NOTES Available in Defense Technical Information Center (DTIC).		
19. KEY WORDS (Continue on reverse side if necessary and identify by block number) detector resolution intensifier minicomputer vidicon data acquisition photomultiplier pixel		
20. ABSTRACT (Continue on reverse side if necessary and identify by block number) With escalating aerospace ground testing costs, it has become imperative to reduce test duration and yet maintain the quantity and quality of test data. Because many of the non-perturbing flow diagnostic techniques developed at AEDC require a measurement of either induced or spontaneous emitted radiation, data acquisition time can be reduced if the spatial, spectral, and temporal variations of the radiation can be measured simultaneously. To achieve this reduction in data acquisition time, AEDC personnel have developed two multi-channel radiation detection systems. The details of these two systems and		

UNCLASSIFIED

SECURITY CLASSIFICATION OF THIS PAGE (When Data Entered)

UNCLASSIFIED

SECURITY CLASSIFICATION OF THIS PAGE(When Data Entered)

20. ABSTRACT, Concluded.

an assessment of their capabilities are presented, and recommendations for improvements are made.

UNCLASSIFIED

SECURITY CLASSIFICATION OF THIS PAGE(When Data Entered)

PREFACE

The work reported herein was conducted by the Arnold Engineering Development Center (AEDC), Air Force Systems Command (AFSC), under Program Element 65807F. The results were obtained by Calspan Field Services, Inc., AEDC Division, operating contractor for Aerospace Flight Dynamics Testing at AEDC, AFSC, Arnold Air Force Station, Tennessee, under AEDC Project No. D200-PW (P32M-C4). The Air Force Project Manager was 2nd Lt. Steve Lehr. The manuscript was submitted for publication on June 28, 1983.

CONTENTS

	<u>Page</u>
1.0 INTRODUCTION	5
1.1 Background	5
1.2 The VICS Concept	5
1.3 The MCPMT Concept	6
2.0 DETAILS OF THE VICS	7
2.1 Components	7
2.2 Image Intensifier	8
2.3 Intensifier/Vidicon Coupling Optics	14
2.4 Vidicon System	15
2.5 Vidicon-Computer Interface Assembly	19
2.6 Minicomputer and Data Acquisition Program	22
2.7 Data Output	24
3.0 DETAILS OF THE MCPMT	24
3.1 MCPMT Characteristics	24
3.2 Uncooled MCPMT Mounting	25
3.3 Thermoelectric Cooler	29
3.4 Data Acquisition Methods	29
4.0 PERFORMANCE	31
4.1 VICS	31
4.2 MCPMT	34
5.0 DISCUSSION	37
5.1 Comparison of AEDC Systems and a Commercial System	37
5.2 Methods for Improvement of AEDC Systems	37
REFERENCES	39

ILLUSTRATIONS

<u>Figure</u>	<u>Page</u>
1. VICS Concept	6
2. Block Diagram of the Basic VICS Instrument System	8
3. Sketch of Image Intensifier	9
4. Intensifier Spectral Response	10
5. Intensifier Gain Characteristics	11
6. Relative Radiant Power of ITT P20 Phosphor as a Function of Wavelength	13

<u>Figure</u>	<u>Page</u>
7. CTF Diagram	14
8. Schematic Representation of a Vidicon	15
9. Vidicon Characteristics	16
10. Sketch of Vidicon Target Area and Standard Scan	18
11. LN ₂ Cooler System for Vidicon	19
12. Block Diagram of Vidicon-Computer Interface Assembly	20
13. Formats of the Command and Data Words for the Vidicon- Computer Interface Assembly	20
14. Timing Diagram of Vidicon Charge Readout Sequence	22
15. Schematic of MCPMT, F4149	25
16. MCPMT Sensitivity as a Function of Wavelength	26
17. Electrical Schematic of MCPMT	26
18. Gain and Dark Current as a Function of Applied Voltage	27
19. Aluminum Housing for MCPMT	28
20. Initial Anode Wiring Configuration	28
21. Thermoelectric Cooler for MCPMT	29
22. Analog and Photon Counting Data Acquisition Methods	30
23. Gated Integration Data Acquisition System	30
24. Linearity Measurement of VICS	34
25. Linearity Measurements of MCPMT	35
26. Integral Photoelectron Count Distribution of MCPMT	36
27. Wavelength Scan Profiles of Two 30-Anode Groups of the MCPMT	37

TABLES

1. Comparison of Multichannel Detection Systems	38
NOMENCLATURE	40

1.0 INTRODUCTION

1.1 BACKGROUND

Many of the nonperturbing flow diagnostic techniques developed at the Arnold Engineering Development Center (AEDC) for the measurement of species density, temperature, and particle size require the observation of emissions generated by the interaction of some form of injected energy with the gas molecules/particles of the flow field under study. Observation of the spectral characteristics of the emitted radiation then reveals information concerning the identity of the constituents, their concentration and temperature, or their size. Generally the emitted radiation is of low intensity and is most often detected with a high gain photomultiplier tube (PMT) coupled to a grating spectrometer. Although extreme sensitivity and excellent spectral resolution can be obtained readily with such an assembly, its operation is speed limited by virtue of mechanical scanning features of the grating drive assemblies. Furthermore, only single "point" measurements are possible, because spatial discrimination at the photocathode is not inherent in regular PM tubes. Therefore, rapid measurements of spatial, spectral, and temporal effects of the radiation processes are difficult to achieve simultaneously.

Certainly the problem can be solved in part for particular experimental cases. For instance, a polychromator arrangement can be used to achieve wide spectral coverage, but spatial measurements would have to be achieved by mechanically repositioning either the excitation beam or the detection system, or both. Unfortunately, this type of arrangement can still result in the waste of expensive test time, and the fixed relative positions of the detectors do not provide very flexible spectral coverage.

The problem has been addressed at AEDC by developing two different detection systems. One detector is called the vidicon-intensifier coupled system (VICS), and the other detector is called the multichannel photomultiplier tube (MCPMT). Both systems are now operational at AEDC for use with electron beam fluorescence, laser-induced fluorescence, laser-Raman, coherent anti-Stokes Raman, and Mie scattering diagnostic techniques. Details of these two systems, their operational modes and characteristics, their performance, and their relative advantages and disadvantages are presented in this report.

1.2 THE VICS CONCEPT

Shown in Fig. 1 is a schematic drawing of the VICS concept. Radiation from the scattering/excitation volume is imaged onto the input slit of a spectrometer which spectrally disperses the input slit images across the face of an image intensifier. A coupling lens between the intensifier output and the vidicon focuses the slit images onto the vidicon face.

At the vidicon the light images are converted to electronic signals that can be stored and then processed by a minicomputer. Because of its two-dimensional and charge storage features, VICS provides the following simultaneous data acquisition capabilities:

- a. spatial variations of the radiation at the spectrometer slits
- b. data gating to obtain time-resolved or time-averaged measurements
- c. data storage for signal time integration
- d. spectrally resolved intensity measurements

In addition, if the spectrometer is replaced with an optical filter system, two-dimensional spatial-spatial measurements are possible.

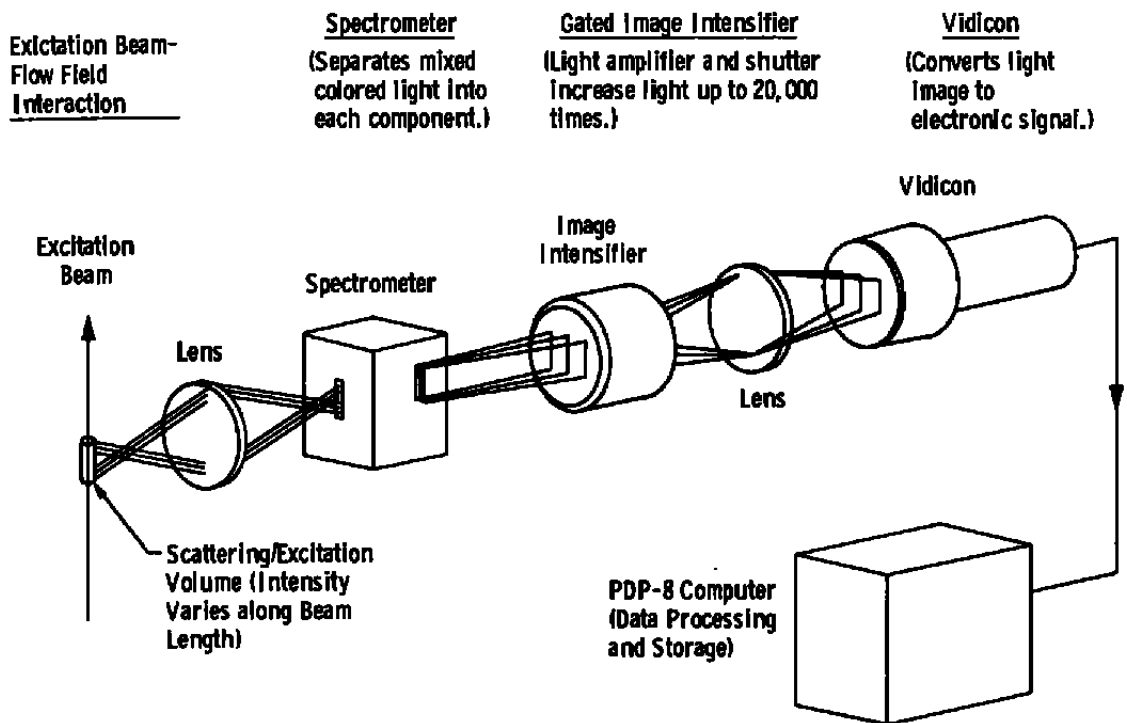


Figure 1. VICS concept.

1.3 THE MCPMT CONCEPT

For many flow diagnostic situations the VICS system does not have the required sensitivity and provides greater spectral/spatial resolution than is actually needed. For these cases the ideal detection system should have the sensitivity and gain of a photomultiplier tube and yet have the multichannel capability needed for spatial and spectral resolution.

International Telephone and Telegraph Corp. (ITT), Surface Sciences Laboratories (SSL), and Instrument Technology, Ltd. (ITL) have recently marketed devices that approach this ideal detection system. All these devices use stacked microchannel plates to achieve high electron gain (10^6 to 10^7), but resolution is achieved by two different methods. The SSL and ITL devices are commonly called "imaging photon detectors." When a single photon strikes the photocathode, a photoelectron is accelerated toward a stack of microchannel plates, producing an output pulse of approximately 10^6 electrons which strikes a resistive anode at a location which has a one-to-one correspondence with that of the original photon. Proximity focusing is used in the photocathode-microchannel plates and microchannel plate-anode gaps. The pulse of charge is collected by four orthogonal electrodes, and position-computing electronics then calculate the location of the charge pulse from ratios of the charge collected at each of the electrodes. Readout is accomplished with an integrating display device such as a storage oscilloscope or computer. These devices are inherently slow and would therefore not be useful for laser scattering applications with pulsed laser sources. The ITT devices (F4149, multichannel photomultiplier tube) replace the resistive anode with a 10 by 10 array of discrete output anodes. Therefore, the performance of the F4149 is equivalent to 100 separate photomultiplier tubes with a total tube volume of less than 10 cm³.

2.0 DETAILS OF THE VICS

2.1 COMPONENTS

The principal components of VICS include the following:

- a. spectrometer with collection optics
- b. intensifier high voltage power supply with remote gating feature
- c. vidicon, vidicon cooler assembly, and vidicon power supply and control system
- d. intensifier-vidicon coupling optics
- e. vidicon-computer interface
- f. PDP-8 minicomputer system

These components are shown collectively in Fig. 2. The collection optics are generally configured to the particular application, but the solid angle of the imaging optics used to focus the observation volume on the spectrometer entrance slit is always matched to the spectrometer solid angle. The spectrally dispersed light is amplified by the intensifier, and the intensifier output is detected by the vidicon target. Individual target charge samples which are proportional to the light intensity at discrete x-y positions on the target are read

according to the x-y deflection coil currents and readout strobes as supplied by the vidicon control unit. The vidicon-computer interface assembly selects the sample position and time of readout by way of the vidicon control unit. Ultimate control actually originates at the computer, and the interface assembly receives information from the computer which specifies the target scanning patterns, the time of vidicon charge readout, and digital conversion.

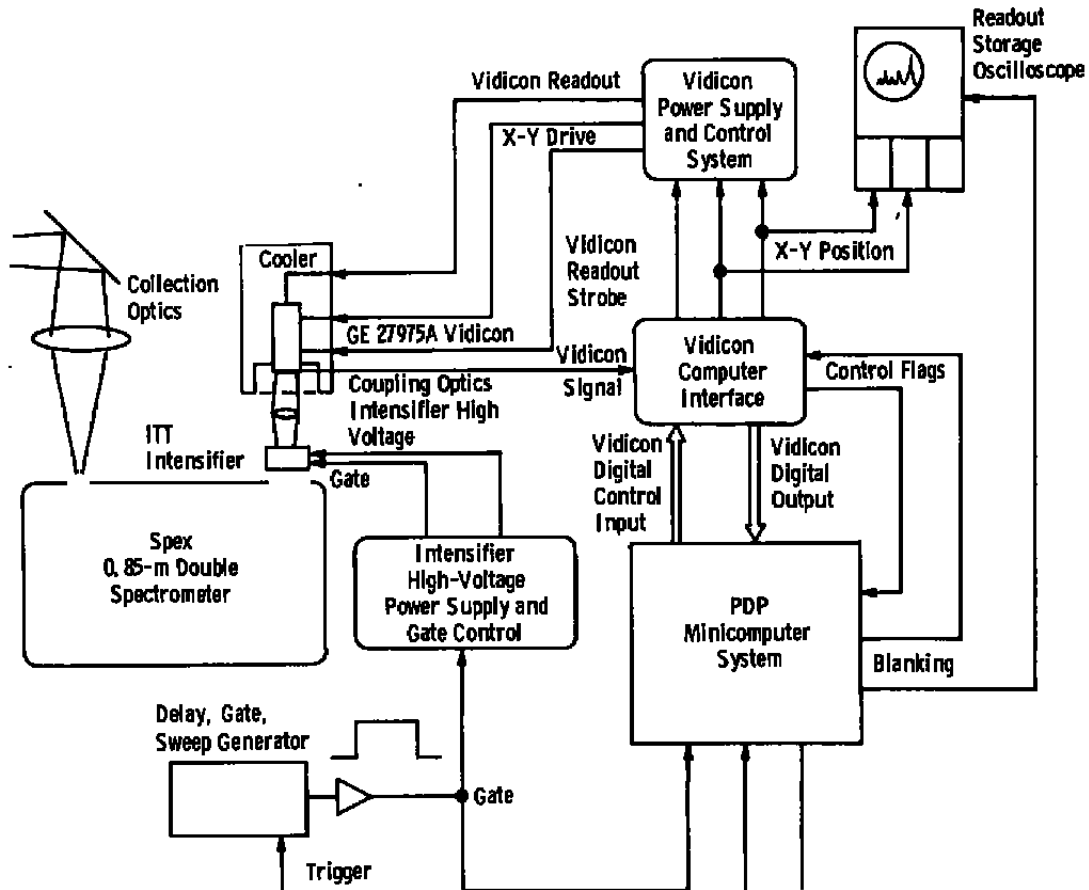
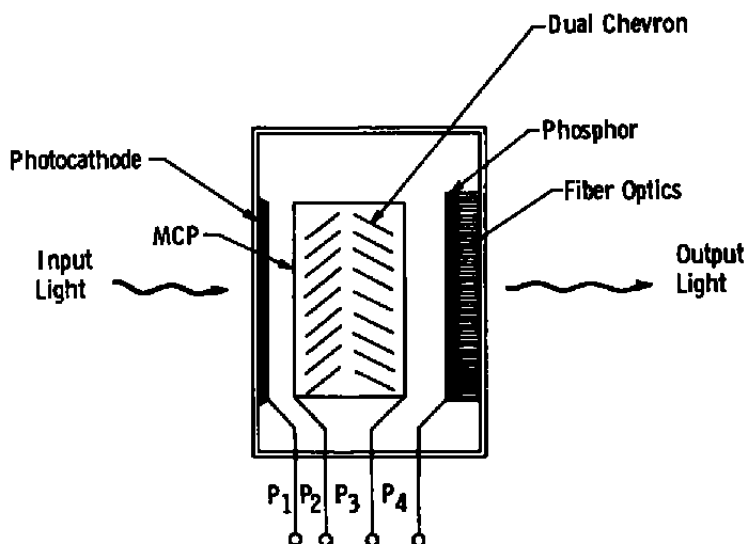


Figure 2. Block diagram of the basic VICS instrument system.

2.2 IMAGE INTENSIFIER

The image intensifier used for this application is formally referred to as a dual-microchannel plate proximity-focused intensifier tube. A sketch of the intensifier is shown in Fig. 3. The microchannel plate (MCP) is a disk-shaped, continuous dynode electron multiplier. The MCP consists of millions of microscopic hollow-glass conducting channels fused into an array. The glass channels are connected in parallel electrically by metal electrodes on opposite faces of the disk. The MCP is specially processed to produce

secondary electrons from the channel surfaces. Therefore, when single electrons generated by light striking the photocathode impinge on the input of the MCP, secondary electrons are generated. These secondary electrons are accelerated by the voltage applied between the disk faces, and they collide with the channel surfaces to dislodge secondary electrons, thereby producing electron multiplication (amplification). In many MCP image intensifier applications, the phosphor viewing screen is placed in close proximity to the output of the MCP, whence the term "proximity-focused" intensifier tube.



P₁ - Photocathode (neg.) - To 1880 Volts

P₂ - MCP Input (neg.) - To 1700 Volts

P₃ - MCP Output (gnd.) - 0

P₄ - Phosphor (pos.) - To 5000 Volts

Figure 3. Sketch of image intensifier.

From Fig. 3 it may be noted that the channels are schematically shown with a chevron notation, illustrating the fact that the channels are at a bias angle with respect to the parallel input and output surfaces. Typical values of this bias are from 5 to 8 deg with respect to the plate surfaces. The function of the bias angle is to reduce ion feedback, increase the probability of secondary electron impact with the channel surface, and reduce direct light feedback from the output phosphor. It should be noted that in the dual-MCP, the two microchannel plates are placed approximately 1 mil apart with their bias angles opposing.

The image intensifier used for VICS was manufactured by ITT, and important descriptive characteristics of the intensifier are given as follows:

- S-20R (extended red) 18-mm-diam photocathode with 7056 glass input window
- P20, 18-mm-diam phosphor with a fiber optic output window
- resolution (ℓ_p) of approximately 22 ℓ_p /mm
- electron gain (G_e) of 6.3×10^4 with a dark current density less than 7×10^{-11} amps/cm²

The spectral response (R_{ia}) of the intensifier is given in Fig. 4 in terms of milliamps/watt. These values can be converted to quantum efficiency (q_e) using the following relation from Ref. 1.

$$q_e(\lambda) = \frac{1.23985 \times 10^2 R_{ia}}{\lambda} \text{ percent} \quad (1)$$

with R_{ia} in units of milliamps/watt and λ in nanometers. From Eq. (1) the peak quantum efficiency is calculated to be approximately 12 percent at 500 nm. Also shown in Fig. 4 is the luminous sensitivity (Φ_i) of the intensifier, 174 μ amps/lumen with the luminous flux input from a 2854°K color temperature tungsten lamp.

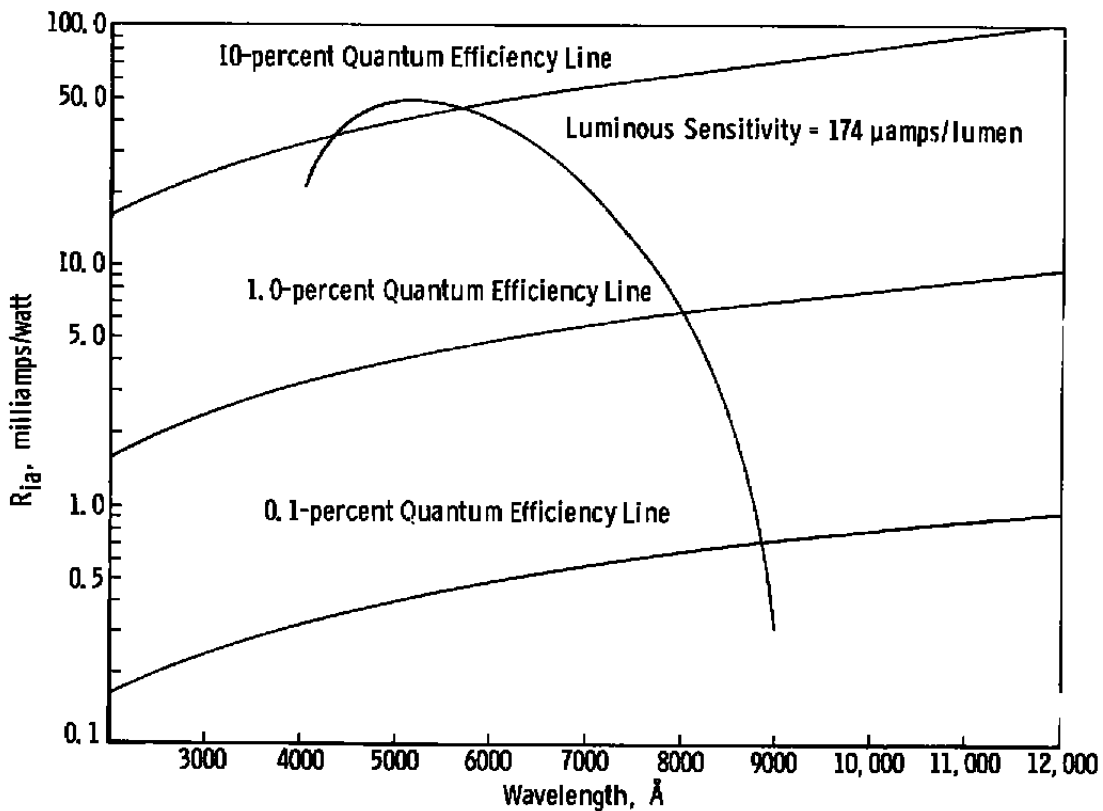


Figure 4. Intensifier spectral response.

The gain characteristics of the intensifier are given in Fig. 5 as a function of the MCP voltage. The electron gain (G_e) is the number of electrons generated by the MCP per input secondary electron from the photocathode. The brightness gain (G_B) is the ratio of the total luminous flux from the phosphor screen to the total luminous flux from a 2854°K standard lamp. The maximum G_B is 5.5×10^6 .

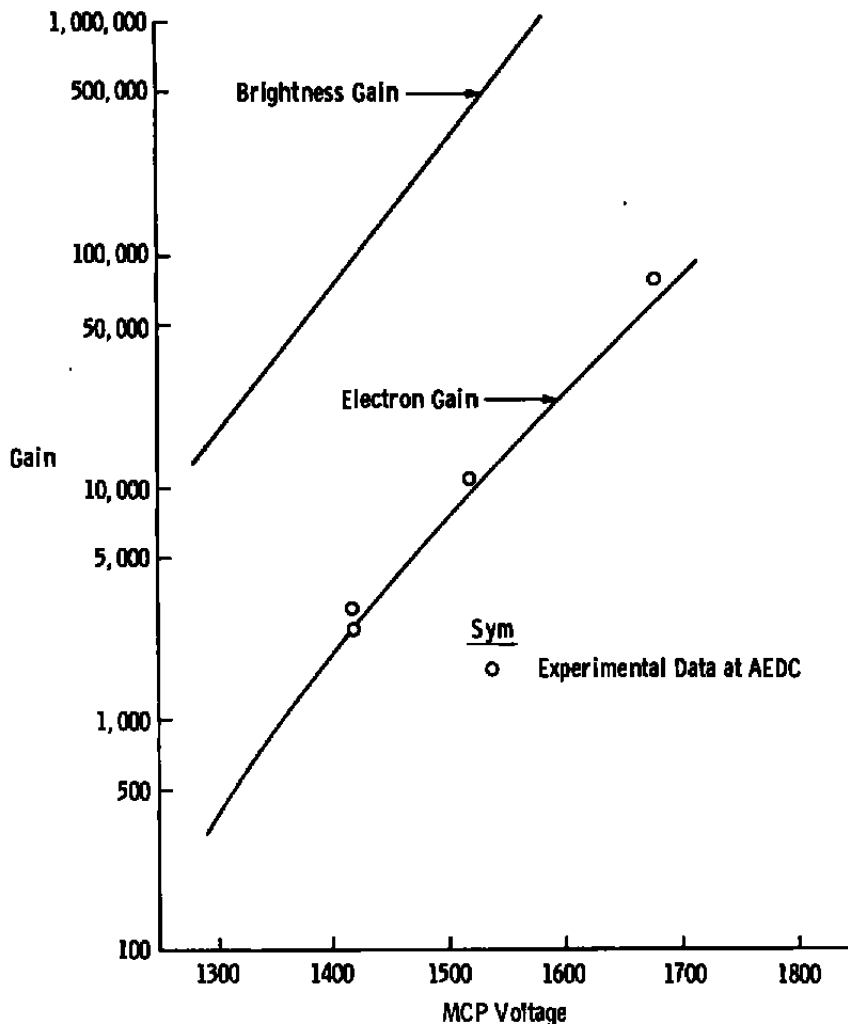


Figure 5. Intensifier gain characteristics.

Another important performance characteristic of the intensifier is the equivalent background input (EBI). The EBI is defined as that amount of illuminance (lumens/cm²) that produces a signal just equal to the noise level. For the VICS intensifier, $EBI = 2.6 \times 10^{-13}$ lumens/cm² at $G_B = 1.3 \times 10^6$.

An additional intensifier parameter of interest is the photon gain (G_p), which is defined as the number of photons from the output phosphor per photon at the photocathode. Photon gain may be calculated using the following relation from Ref. 2.

$$G_p = q_e(\lambda) V E G_c \quad (2)$$

where

V = the effective accelerating voltage, ev
 E = the photon conversion efficiency of
the phosphor (output photons/
electron/ev of output photons)

Effective accelerating voltage is used rather than the electron accelerating potential (5000 volts), because the negative ion feedback film energy loss is approximately 2500 volts. This loss is sometimes referred to as "dead voltage." The maximum effective accelerating voltage is therefore 2500 volts.

The P20 phosphor emits radiation over a rather narrow spectral range (see Fig. 6), and the peak response is at 525 nm with a nominal lifetime of 60 μ sec. The mean photon energy (\bar{E}_p) from the phosphor is 2.4 ev. The phosphor efficiency is

$$E' = \frac{\text{watts of radiated light from phosphor}}{\text{watts of electron energy dissipated in the phosphor}}$$

If we define another efficiency factor,

$$E'' = \frac{\text{number of photons out}}{\text{number of electrons in}}$$

then $E'' = E'(V_p/\bar{E}_p)$

where

V_p = mean energy of the electrons, ev

The phosphor efficiency used in Eq. (2) is therefore

$$E = \frac{E'}{\bar{E}_p} \quad (3)$$

For the P20 phosphor it is nominally found (Ref. 2) that

$$E \approx 0.075$$

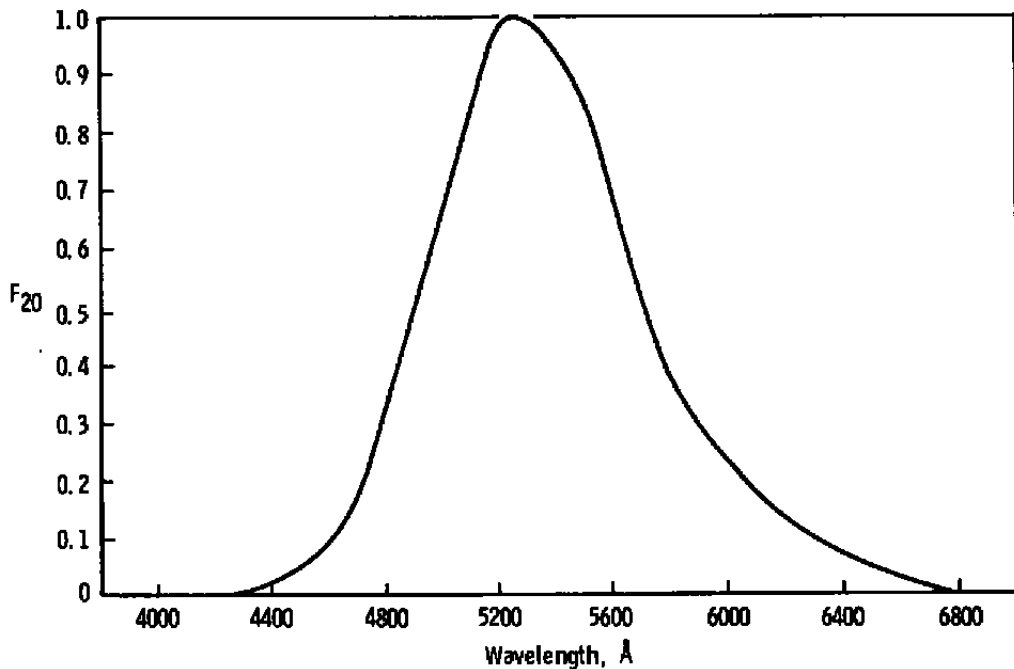


Figure 6. Relative radiant power of ITT P20 phosphor as a function of wavelength.

The previously stated resolution of the intensifier is $\ell_{pi} = 22 \ell_p/\text{mm}$. If a pixel is defined as the smallest resolvable picture element, then the intensifier pixel size is (from Ref. 3)

$$d_i = \frac{1}{2\ell_{pi}} = 0.023 \text{ mm} \quad (4)$$

The limiting resolution definition used by ITT (Ref. 3) corresponds to a contrast transfer function (CTF) of 8.9 percent. The CTF is defined as the square-wave spatial-frequency amplitude response. Amplitude response is frequently quoted in this form because it is easy to measure by using a black and white bar chart for a test pattern giving 100-percent contrast. The luminance pattern of the bar chart and the output of the intensifier are shown in Fig. 7. The contrast transfer function is defined as

$$\text{CTF} = \frac{Q}{P} \quad (5)$$

where

Q = maximum-minimum signals

P = maximum signal

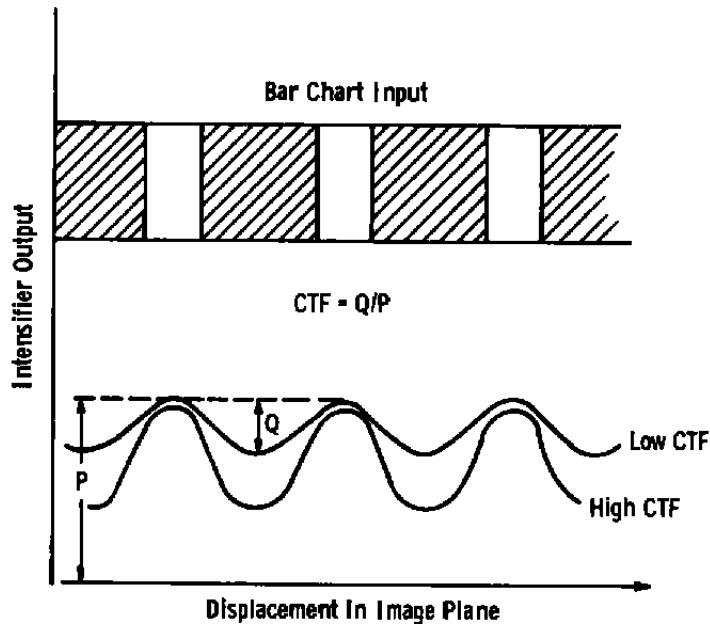


Figure 7. CTF diagram.

Gating of the intensifier can be accomplished by pulsing the photocathode relative to the input of the microchannel plate assembly. High voltage isolation is accomplished using an opto-isolator. During the time the intensifier is turned off, the photocathode is approximately 40 volts positive with respect to the MCP. During the gating interval, the photo-cathode drops to the negative high voltage input line through a high voltage transistor. The minimum gate width attainable with the present method is approximately 6 μ sec. The maximum gain for this assembly is obtained with - 1880 volts input.

2.3 INTENSIFIER/VIDICON COUPLING OPTICS

The intensifier output is coupled to the vidicon target with a SAPHIR six-element, f # 1.4, 50-mm-diam lens. The magnification (M), which is really a reduction in this case, of the lens is 0.6. The coupling efficiency (c_e) of the lens is defined as

$$c_e \equiv \frac{\text{No. of photons per unit area from the phosphor}}{\text{No. of photons per unit area incident on the vidicon}}$$

$$c_e \text{ (Ref. 10)} = \frac{\eta_{cl}}{4(f\#)^2 (1 + M)^2} = \frac{\Omega_{cl} \eta_{cl}}{\pi M^2} \quad (6)$$

where Ω_{cl} = the solid angle of the coupling lens

and

η_{cl} = the mean transmittance of the lens system
for the spectral range of the P20 phosphor

With $\Omega_{cl} = 0.056$ and assuming $\eta_{cl} \approx 0.9$,

$$c_e = 0.045$$

Therefore, the intensity of the phosphor is reduced by a factor of 22.2 by the coupling lens.

2.4 VIDICON SYSTEM

The imaging device used for the VICS system is a silicon diode vidicon. A schematic representation of a vidicon is given in Fig. 8. The vidicon utilizes an electron beam to scan the photoconductive target, an array of silicon photodiodes, in which the charge distribution produced by the optical image coupled from the intensifier onto the input side of the target represents the integrated light intensity since the last readout. The current accepted from the scanning beam by each point on the target (to restore the target to its original potential) constitutes the output video signal.

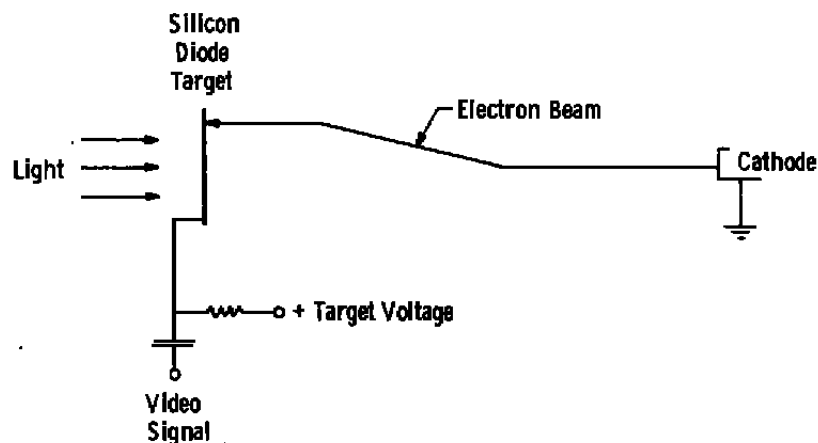


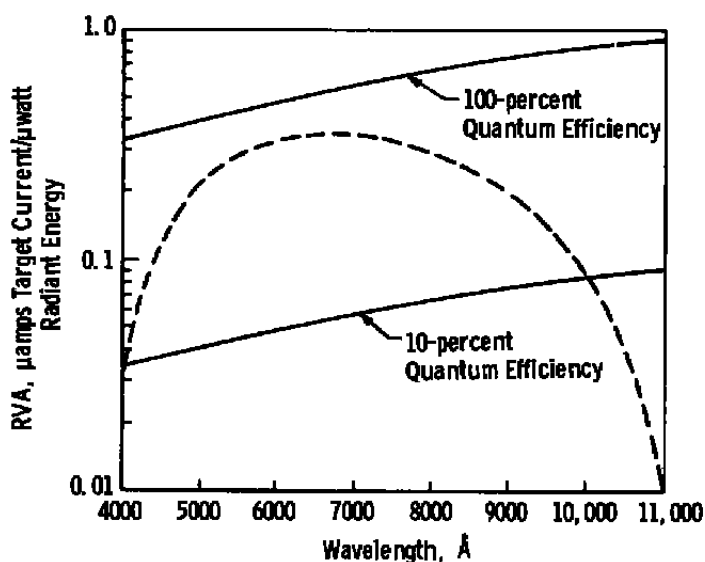
Figure 8. Schematic representation of a vidicon.

The vidicon presently used for VICS is a General Electric 27975A EPICON. Important descriptive characteristics of the vidicon are given below.

- a. 0.625-in. (15.875-mm) target diameter with a 0.375-in. (9.525-mm) by 0.5-in. (12.7-mm) raster
- b. 400- to 1000-nm spectral response with quantum efficiency greater than 10 percent
- c. magnetic focus and deflection
- d. resolution (R_{TV}) of 700 TV lines at a CTF of 8.9 percent

The spectral response curve of the vidicon is given in Fig. 9a, and it can be seen that the absolute response (R_{va}) at 5250 Å (the phosphor peak) is

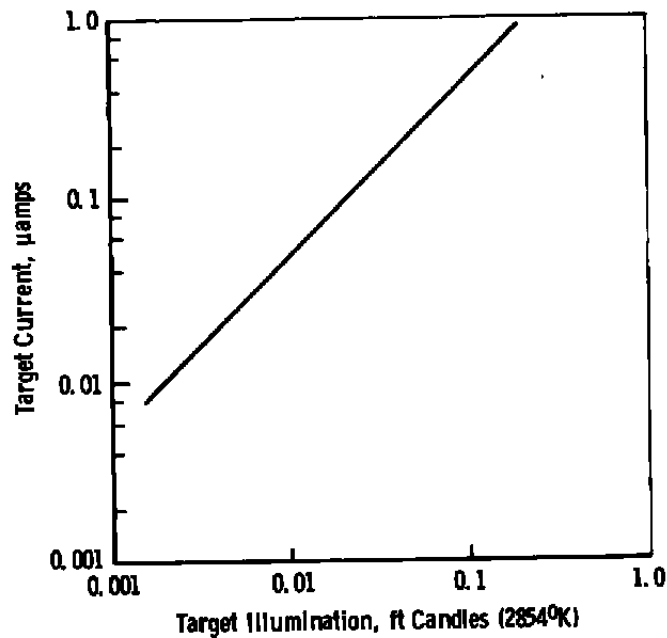
$$R_{va} \approx 0.25 \text{ } \mu\text{amps}/\mu\text{watt of radiant energy}$$



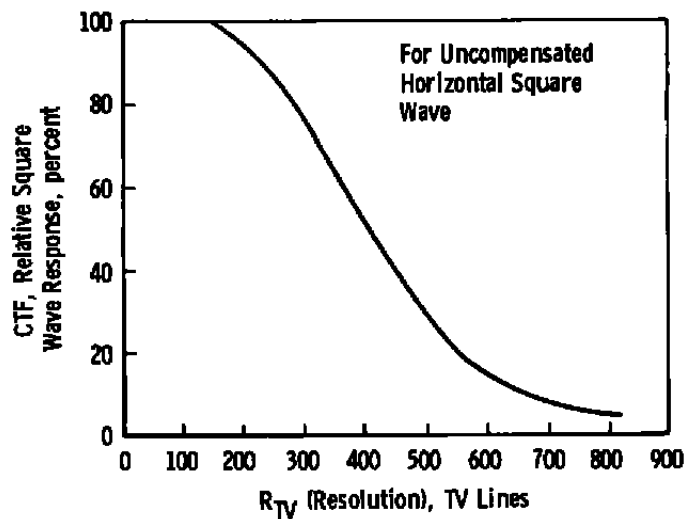
a. RVA as a function of wavelength

Figure 9. Vidicon characteristics.

The full spectrum response (R_{VFS}) obtained using a tungsten strip standard lamp at 2854°K is given in Fig. 9b. The CTF versus resolution in TV lines is given in Fig. 9c. Rather than use resolution in TV lines, it is preferred to use resolution of the vidicon in line pairs/mm (ℓ_{pv}). Shown in Fig. 10 is a sketch of the vidicon target area with the standard scan or picture raster with a 4:3 aspect ratio. R_{TV} is the number of TV lines, or full cycles, per raster height;



b. Full spectrum response of vidicon
Figure 9. Continued.



c. Vidicon resolution
Figure 9. Concluded.

therefore, the number of scan lines (full cycle) per raster diagonal (R'_{TV}) at 8.9 percent CTF is (from Ref. 3),

$$R'_{TV} = \frac{R_{TV}}{1.2} = 583.3 \quad (7)$$

The resolution in line pairs/mm is then

$$\ell_{pv} = \frac{R'_{TV}}{D} = 36.7 \text{ line pairs/mm} \quad (8)$$

Therefore, the minimum pixel size for the vidicon is

$$(\text{pixel})_{vmin} = \frac{1}{2\ell_{pv}} = 0.0136 \text{ mm} \quad (9)$$

The vidicon is mounted within a Products for Research, Inc. Model TE-203TS-RF liquid nitrogen (LN_2)-cooled housing. The cooling system is shown in Fig. 11. A 100- ℓ dewar supplies the LN_2 , and the controlling mechanism provides for continuously adjustable vidicon temperature over the range from 0 to -100°C . The system can maintain the vidicon at a nominal operating temperature of -60°C for at least 100 hours of continuous operation, and at this temperature the vidicon dark current is approximately 9.6×10^{-12} amps.

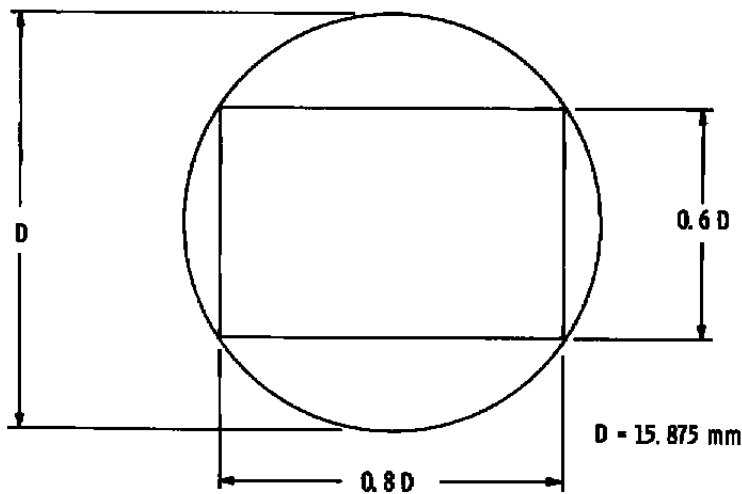


Figure 10. Sketch of vidicon target area and standard scan.

The assemblage of components in Fig. 2 denoted Vidicon Power Supply and Control System contains the power supplies for the static electron beam controls including the filament, grid, and focusing and acceleration anodes. The x-y drive circuits for the deflection coils are also included and serve as buffer circuits for externally supplied readout position control. These control functions are capable of random access to individually selected vidicon target positions. The vidicon readout requires only the application of an acceptable pulse to turn on the electron beam. The necessary pulse duration was chosen

experimentally, taking into consideration such things as percentage target position discharge, noise, linearity, offset, etc. The vidicon control system conditions the pulse (known as the vidicon readout strobe), and performs all level-shifting and pulse-shaping functions required by the vidicon.

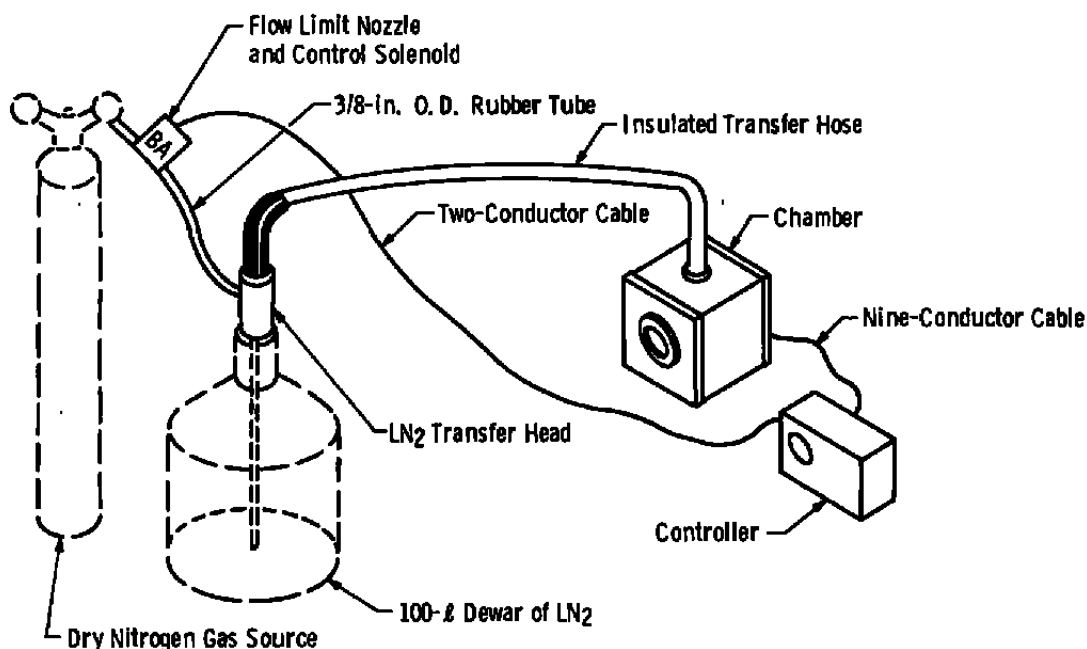


Figure 11. LN₂ cooler system for vidicon.

2.5 VIDICON-COMPUTER INTERFACE ASSEMBLY

All vidicon operations are under computer control and are executed through a twelve-bit I/O buffer. The vidicon power supply-control device discussed above is basically a slave unit and serves as a buffer for functions originating from the vidicon-computer interface assembly. Thus the interface assembly serves to execute commands for the vidicon, select vidicon readout positions, and process target current for digital input to the processor. A block diagram of the vidicon-computer interface assembly is shown in Fig. 12.

There are three main sections of the interface assembly: (1) control, (2) vidicon target position selection, and (3) pixel charge readout and conversion. The computer commands control all vidicon operations by implementing target preparation, target readout position specification, data input and conversion, and interface control. The computer input word similarly contains interface converter output data and certain status flags. The command format and codes are shown in Fig. 13.

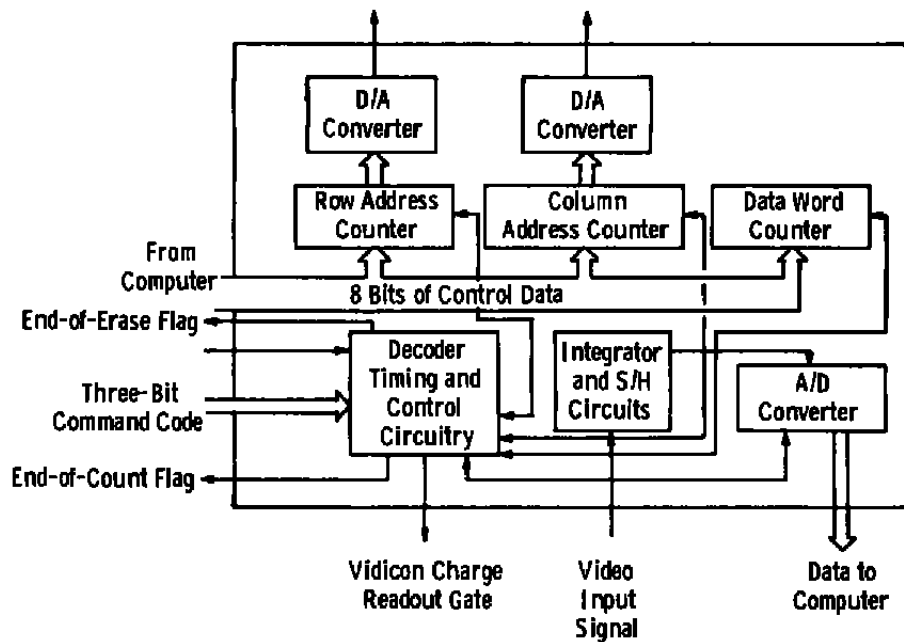
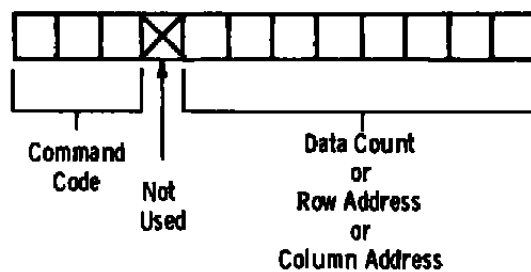
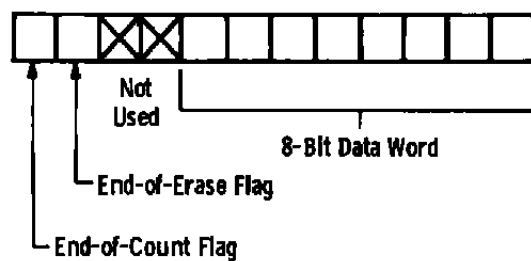


Figure 12. Block diagram of vidicon-computer interface assembly.



Command Codes: 0 - Load Row Address
 1 - Load Column Address
 2 - Load Data Count
 5 - Single-Cycle Erase
 6 - Multicycle Erase

a. Command word for mat



b. Data word format

Figure 13. Formats of the command and data words for the vidicon-computer interface assembly.

In general, the following operational sequence is used:

- a. During intervals of no data acquisition, the continuous erase mode is in effect.
- b. Just before data acquisition, a single frame erase is put into effect which finishes the erase of the current frame.
- c. Data are then transferred to the interface, and the next readout position and sample count for subsequent readout cycle are specified.
- d. Readout strobes are started and continued until the sample counter is decremented to zero. Each readout is accompanied by an automatic advance to the next horizontal vidicon target position.
- e. Steps c and d are repeated according to the number of target zones to be read.
- f. Upon completion of data input, an erase may again be initiated in preparation for the next input sequence.

Erasure is nothing more than the removal of thermally generated charge by a readout sequence where the specified zone is the entire target assembly and the data word readout and the associated synchronization are not applicable.

For low signal operations requiring a long exposure time, a special filament switching step is substituted for step b and is called step b'. The purpose of this step is to eliminate backlighting of the vidicon target by the filament. Step b' is as follows:

- b'. Six frame erases are put into effect, and then the filament is switched off by the computer. Two more frame erases are executed to allow the filament to cool. Intensifier exposure is then permitted for a preset time duration. The filament is then switched back on, and, after a 10-sec delay to allow the filament to reach operating temperature, the vidicon readout proceeds as previously noted by steps c, d, and e.

The vidicon target area is divided into 65,536 pixels, equivalent to 256 resolution elements on a side. The interface unit contains two eight-bit bipolar digital-to-analog (D/A) converters for positioning the beam. The digital inputs to the x-y deflection D/A converters originate from two four-bit IC counter-registers which in turn are loaded from the computer I/O buffer. These devices are normally in the counter mode as required for data readout or target erasure-preparation. These eight-bit counters are connected as a 16-bit counter with a carry from x to y. Normally the counter advance is applied to the horizontal registers although the x-y coils can be interchanged in such a way that vertical scanning is also possible.

The vidicon target output pulse is integrated in a gated integrator circuit to give an output proportional to total accumulated charge. A vidicon readout pulse is sent to the control grid simultaneously with the gate pulse which is applied to the integrator. This initiates a series of data collection and conversion sequences which in effect constitute a readout cycle for an individual vidicon pixel. A timing diagram is shown in Fig. 14. During the time of integration, the track mode is selected for a sample-and-hold amplifier which is subsequently allowed to sample the integrator's final value before it is reset. The vidicon address counters are advanced immediately after the vidicon gate is terminated so that the vidicon deflection coils are completely stabilized before the next sampling sequence. Digital conversion is initiated immediately after the sample-and-hold amplifier switches to the hold mode. Using the overall timing cycle shown, an 83-kHz sampling rate (12- μ sec sampling time) can be obtained.

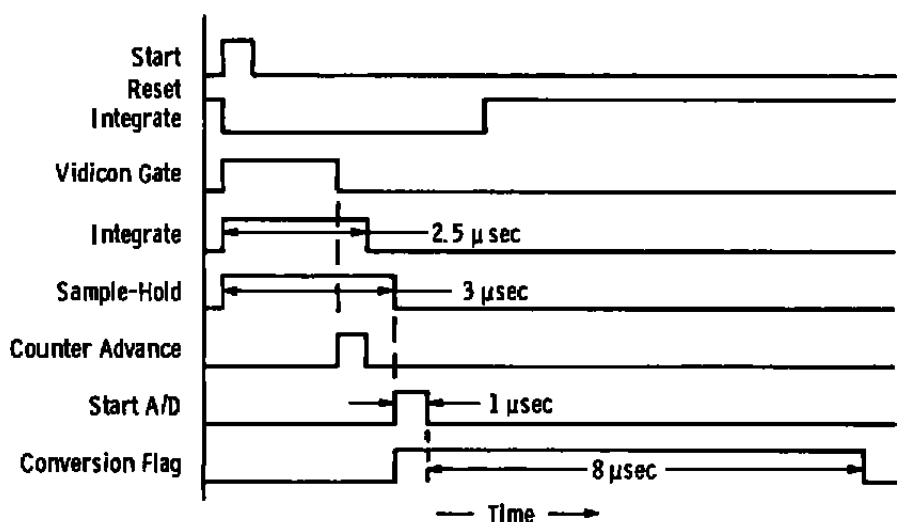


Figure 14. Timing diagram of vidicon charge readout sequence.

2.6 MINICOMPUTER AND DATA ACQUISITION PROGRAM

The minicomputer is the hub of the VICS system. Adapting the computer to many applications requires a nucleus of systems software routines that allow the user to avoid the details of the operation of the vidicon system. Such a set of routines was designed for the system and is called the Minicomputer-Based Image-Intensifier-Vidicon System Software (MIIVSS). MIIVSS was designed to control all vidicon operations and the acquisition, storage, and retrieval of data (Ref. 4). The user software calls MIIVSS routines to perform the necessary vidicon operations; the order of such calls, under certain restrictions, is left to the user for definition.

The primary functions of MIIVSS are as follows:

- a. controlling the test mode operation of the vidicon system
- b. inputting data from the vidicon system, storing data in files on disk, and retrieving data for display and reduction
- c. defining the format of files
- d. retaining the locations of files on disk
- e. opening and closing files, and deleting files from storage
- f. detecting and tracing errors

Data are read from the vidicon target in rectangular patterns called "fields". Fields are rectangular because of the simplicity and speed afforded by the technique. The simplicity arises from the fact that any rectangular geometry can be specified by the following parameters:

- a. the address of the row and column of the first pixel to be read
- b. the number of pixels to be read from each row
- c. the number of rows to be read
- d. the spacing between rows

The speed arises from the fact that the row address is advanced automatically when each pixel is read from the interface, thereby eliminating the need for a computer address reference except at the end of a completed row. The use of rectangular fields does not preclude the reading of other geometries since such patterns can be enclosed within fields and, during data reduction, all data not in the pattern of interest can be ignored. This allows flexibility for use in a wide variety of applications.

Maximum data storage throughput is a necessity for MIIVSS because of the quantity of data that can be acquired by the vidicon system and the problem of noise buildup on the vidicon target. Achieving the necessary speed is impeded by the inherent slowness of the floppy disk system. The data acquisition and storage technique used must take advantage of the speed of the computer and the interface yet take into account the lack of speed of the floppy disk. A minimum access time disk-writing technique was developed for MIIVSS to allow the computer to acquire and store data on the disk at high transfer rates. MIIVSS drives the floppy disk at its fastest rate and performs data acquisition while the disk system simultaneously records data onto the disk.

Simultaneous filling of the disk buffer and writing of its contents onto disk are not possible with the floppy disk. Therefore, adjacent sectors cannot be filled during the same disk revolution. MIVSS fills every second sector during one revolution of the disk and the remaining sectors during the next revolution. While the skipped sector passes the read/write head, the disk buffer is filled and its contents are written into the next sector. Data sufficient to fill a disk sector are read from the vidicon, at which time the contents of the data buffer are transferred to the disk buffer. After the writing on disk has been initiated, new data are again read and transferred to the vidicon data buffer. Thus simultaneous operations of data input and disk data storage are in progress. With this file-writing technique, the data from the entire vidicon target are read and stored in approximately 7.0 seconds. The specially designed file-writing technique has a throughput rate more than an order of magnitude higher than the simple technique of writing sequentially into adjacent sectors.

2.7 DATA OUTPUT

The data from VICS can be presented by several methods. For formal data presentation the vidicon output is presented as a selectable single line sweep of the vidicon face or a single line presentation that is the average of all the vertical pixels for each horizontal position. These data can be observed on a DECscope® screen, and a hard copy can also be produced. Furthermore, digital output is given via a DECwriter® line printer. For informal data presentation (setup, alignment, checkout, etc.) the VICS output can be displayed on a storage oscilloscope (Tektronix 7633) with the vidicon sweeps at an arbitrary free-running speed. For single horizontal line presentation the oscilloscope is in the single sweep storage mode with triggering provided by the start of the vertical sweep, and the vertical input is the signal out of the vidicon preamplifier. For a full screen display the scope is set up for an x-y display with the vidicon preamplifier output fed to the intensity (z) input of the oscilloscope.

3.0 DETAILS OF THE MCPMT

3.1 MCPMT CHARACTERISTICS

A schematic of the F4149 MCPMT is shown in Fig. 15. The input window material is UV-grade fused silica with a nominal 5.1-mm thickness. An S-20 photocathode sensitivity (see Fig. 16) is standard, and the active diameter is 25 mm. A maximum available gain of 5×10^6 is achieved with a face-to-face configuration of three individual straight-channel bias cut microchannel plates stacked in a staggered form and operated with a single overall applied voltage. This configuration is commonly referred to as a z-plate microchannel plate. The electrical schematic of the MCPMT is shown in Fig. 17 with typical and maximum operating voltages. A maximum average current per anode, i_{mx1} , of 10^{-8} amps cannot be

exceeded, but higher peak currents are permissible. The total anode dark current, i_{td} , is specified to be 7.2×10^{-10} amps, which is equivalent to 4500 photoelectron counts/sec, n_{td} , at a gain of 10^6 . A gain and dark current curve for the MCPMT supplied by ITT is shown in Fig. 18.

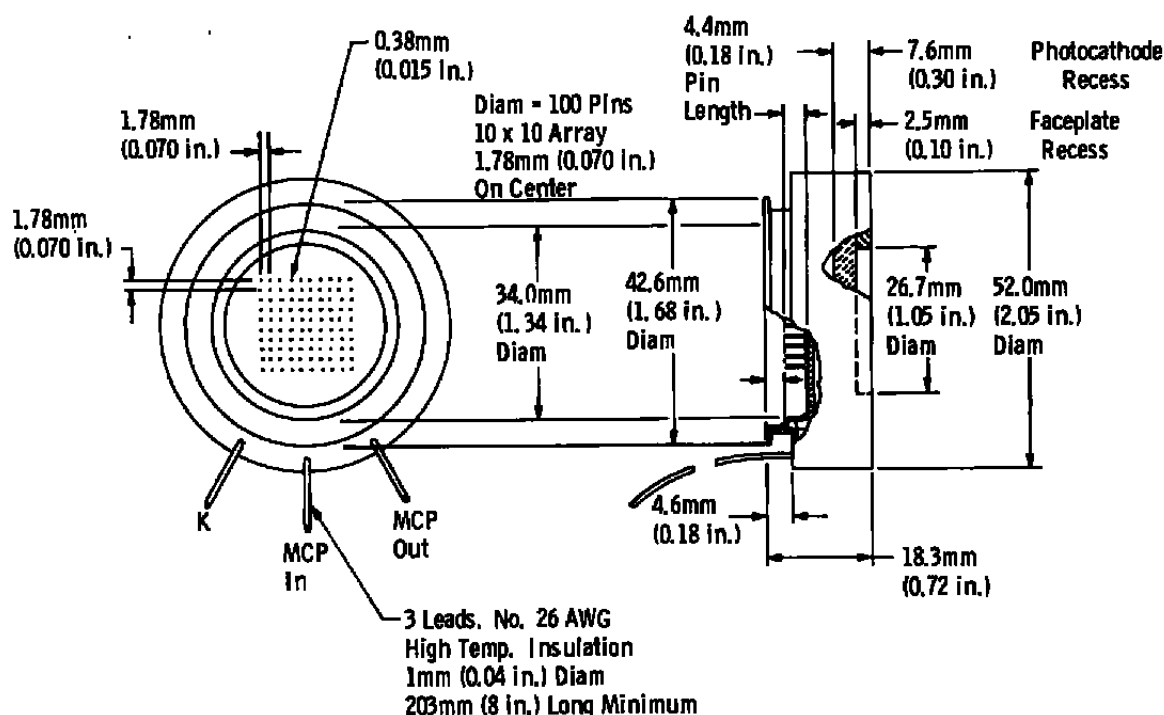


Figure 15. Schematic of MCPMT, F4149.

3.2 UNCOOLED MCPMT MOUNTING

The F4149 was supplied as a potted tube assembly with flying leads, and therefore a suitable mounting had to be fabricated. The initial mount was fabricated from aluminum, and a schematic of the aluminum mount is shown in Fig. 19. This mounting can be attached to a precision optical rotation mount for ease of alignment of the MCPMT to the radiation source upon which measurements are to be made.

Electrical connections to the MCPMT anode pins were made via sliding contacts mounted in a small printed circuit board with a 10 by 10 configuration to exactly match the MCPMT anode pin array. The contacts located at the back of the printed circuit board could then be wired into any desired detector element configuration or combination. The initial wiring configuration is shown in Fig. 20; it consists of two sets of 10 rows and 3

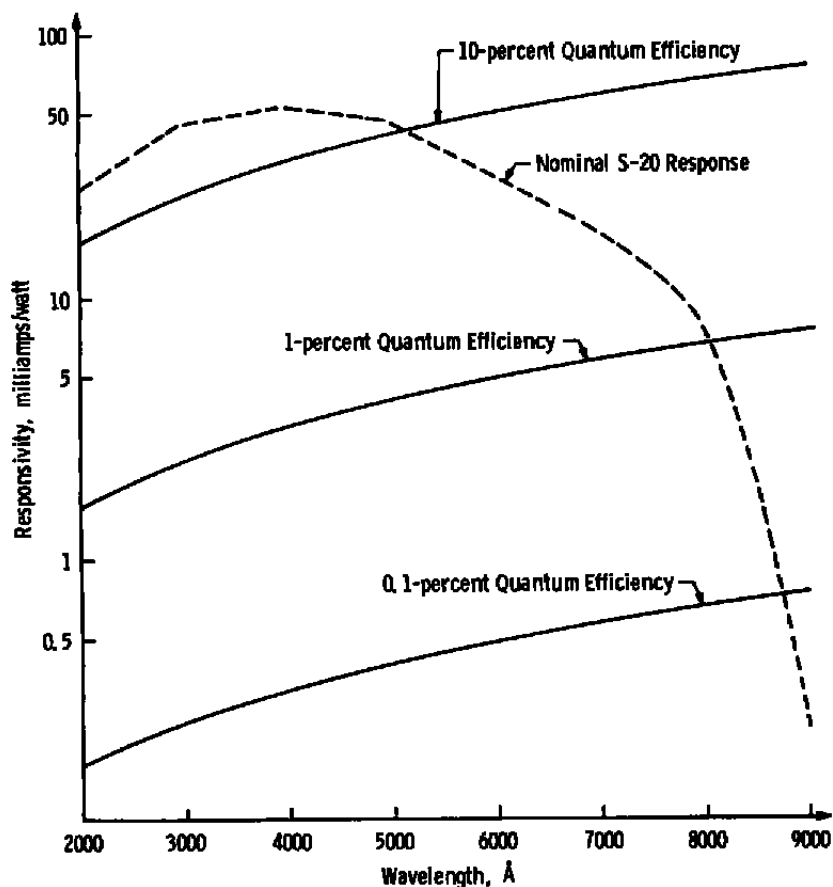


Figure 16. MCPMT sensitivity as a function of wavelength.

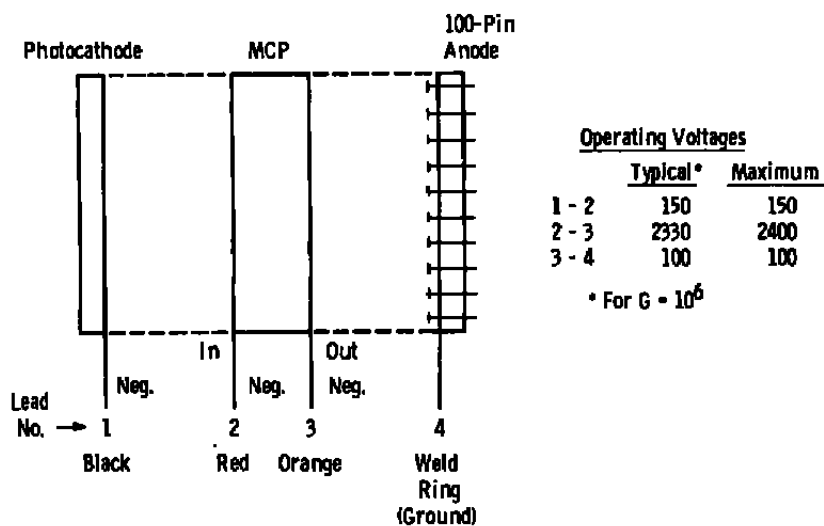


Figure 17. Electrical schematic of MCPMT.

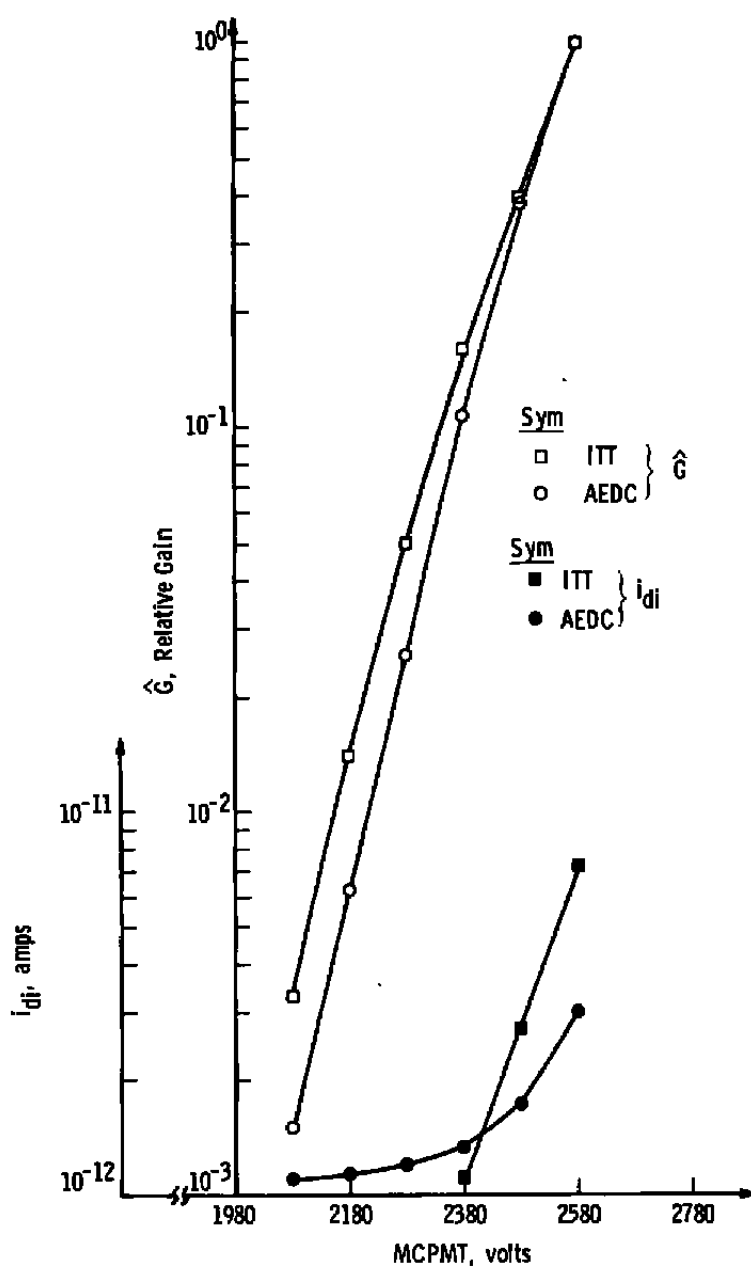


Figure 18. Gain and dark current as a function of applied voltage.

columns connected together, and one group of 10 rows and 1 column. Output wires from the three groups were connected to BNC sockets attached at the rear of the MCPMT mount.

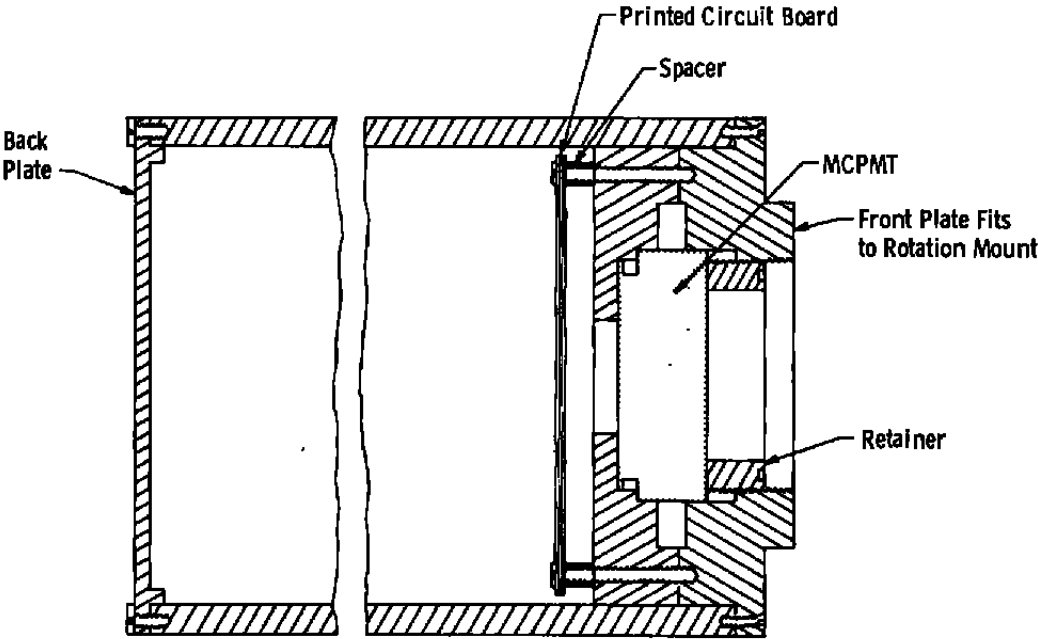


Figure 19. Aluminum housing for MCPMT.

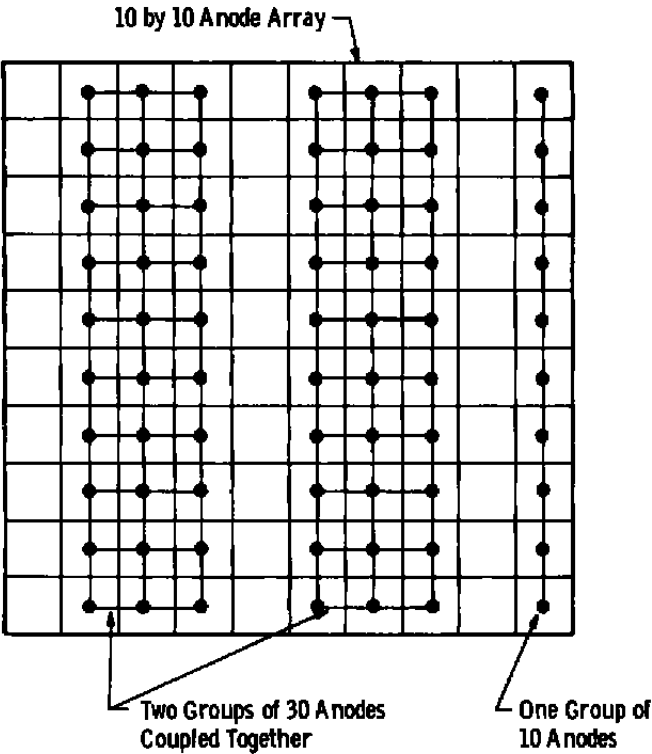


Figure 20. Initial anode wiring configuration.

3.3 THERMOELECTRIC COOLER

For situations of low signal level, the dark current level of the MCPMT can be reduced by cooling. The MCPMT can be mounted in a Products for Research, Inc. Model TE-264TS-RF thermoelectric cooler as shown in Fig. 21. The tube can be cooled to -50°C and held stable within $\pm 0.1^{\circ}\text{C}$ with water used as the heat exchange mechanism. The double pane insulating window is made of UV grade fused silica. Outputs from the MCPMT are available at the rear of the housing, but the number of outputs is presently limited to 19 because of space limitations. With the tube at -50°C the total dark current is reduced by a factor of 40.

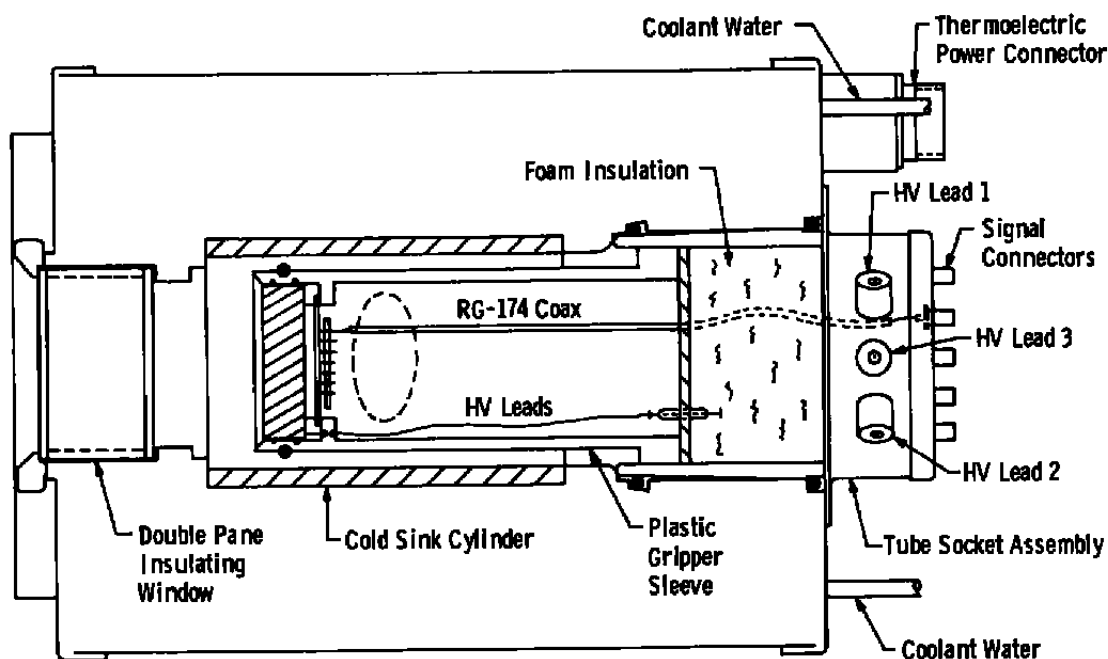


Figure 21. Thermoelectric cooler for MCPMT.

3.4 DATA ACQUISITION METHODS

Readout of the MCPMT can be achieved by the straightforward method of connecting the outputs to electrometers and subsequently to strip chart recorders for spectral display. A single Keithley Model 610B electrometer was used in the laboratory to sequentially monitor the outputs of the initial MCPMT anode configuration (see Fig. 22). For pulsed measurements the output of the MCPMT can be displayed on a Tektronics Model 7633 storage oscilloscope.

For low signal levels, photon-counting electronics can be used for readout of the MCPMT. These electronics consist of a pulse height discriminator, pulse amplifier, counter, and timer for a single data channel. The Ortec photon-counting system shown in Fig. 22 was used in the laboratory to sequentially monitor the MCPMT outputs.

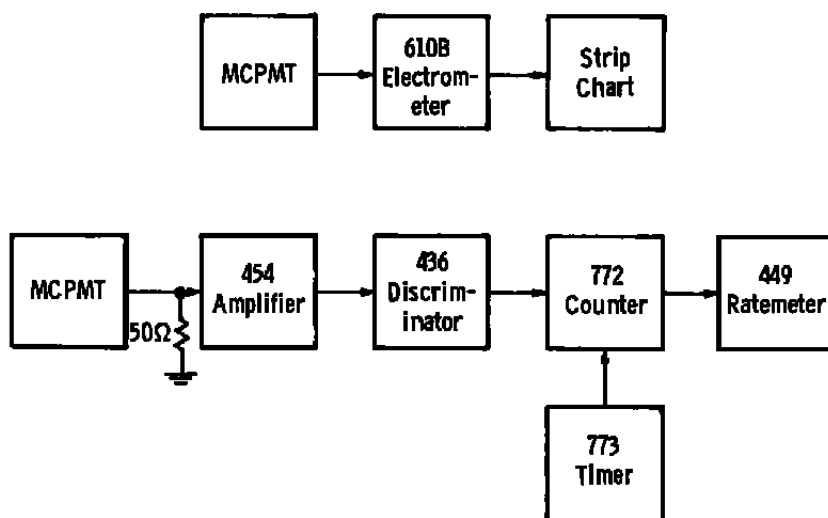


Figure 22. Analog and photon counting data acquisition methods.

A data acquisition system has also been developed for use with the MCPMT for pulsed radiation measurements. The system consists of a Digital Equipment Corporation LSI-11/2 microcomputer equipped with an LA36 DECwriter II terminal, a Kinetic Systems Corporation Model 1500 CAMAC dataway crate with Model 3912-Z1G crate controller, two CAMAC-compatible LeCroy Research Systems Corporation Model 2250L fast-buffered gated-integrator modules, and a simple gating circuit. Figure 23 shows a block diagram of the system.

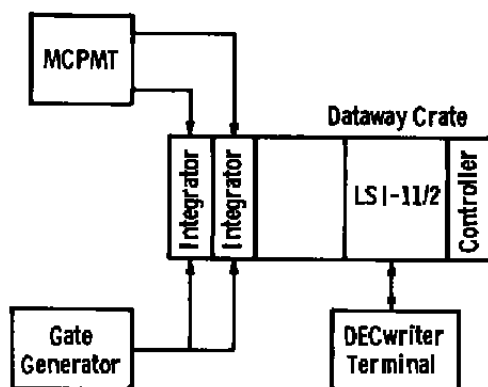


Figure 23. Gated integration data acquisition system.

Each gated integrator module contains twelve independent integrating analog-to-digital converters (ADC's), each of which digitizes to nine bits the amount of charge input at its analog port over the duration of an externally applied common gate pulse. Each channel requires a 10- μ sec cycle time during which the data are digitized and transferred to a 32-deep first-in, first-out (FIFO) memory.

The LSI-11/2 microcomputer resides in the CAMAC crate and receives its power from the crate. It is interfaced with the CAMAC crate through the crate controller, which permits communication with the gated integrator modules over the CAMAC dataway. The LA36 terminal is used for control of the system and printout of the data.

The computer is programmed to perform one scan read of the first ten ADC's of each integrator module. Each ADC can be connected to one of the MCPMT rows with each gated integrator module converting the inputs from one group of MCPMT columns. The data acquisition sequence begins by gating the integrator modules with a gate pulse provided by the gating circuit. The duration of this pulse can be preselected to allow proper integration of the charge without overscaling the ADC's. The computer is then commanded by keyboard input to read the data and print the results with the terminal printer.

4.0 PERFORMANCE

4.1 VICS

Noise level, resolution, and spectral range are three of the most important performance parameters for both these multichannel detectors. As can be seen in Fig. 4 the VICS is limited to the visible spectral range from 3500 to 8500 Å by the intensifier spectral response.

To evaluate the minimum noise level of the VICS, three sources of noise must be included as follows:

1. the vidicon signal generated by the dark level output of the intensifier, i_{di}
2. the thermally generated dark level of the vidicon itself, i_{dv}
3. the noise level output from the video preamplifier of the vidicon, i_{av}

Associated with each of these noise levels is a time interval during which the noise influences a signal measurement, and these intervals are as follows, respectively:

1. the intensifier gate time, τ_{gi}
2. the exposure or optical integration time of the vidicon, τ_{ov}
3. the vidicon pixel readout time, τ_{px}

At present the minimum time to read out the entire vidicon raster area is 7 sec; therefore, $\tau_{ov} = 7$ sec. From Fig. 14 it can be seen that $\tau_{px} = 2.5 \mu\text{sec}$, and the present minimum intensifier gate time is $\tau_{gi} = 6 \mu\text{sec}$ for pulsed mode operation. Assuming a nominal input wavelength of 5000 \AA at the intensifier, the equivalent dark photon input associated with i_{di} is

$$N_{di} = (i_{di})(\tau_{gi}) = 10^{-7} \text{ photons/(pixel)}_i$$

for pulsed mode operation.

The equivalent dark photon input associated with i_{dv} and i_{av} is

$$N_{dv} = (i_{dv})(\tau_{ov}) + (i_{av})(\tau_{px}) = 1.6 \text{ photons/(pixel)}_i$$

The total equivalent dark photon input associated with the VICS for pulsed mode operation is then

$$N_{dvics} (\text{pulsed}) = N_{di} + N_{dv} = 1.6 \text{ photons/(pixel)}_i$$

For continuous mode operation, $\tau_{gi} = \tau_{ov}$, and

$$N_{dvics} (\text{cont}) = 1.7 \text{ photons/(pixel)}_i$$

The minimum acceptable signal-to-noise ratio is defined as

$$(\text{SNR})_{\min} = 10 = \frac{N_s}{2 N_{dvics} + N_s} \quad (10)$$

Therefore, the minimum acceptable exposure for the VICS is

$$N_{s\min} = 103 \text{ photons/(pixel)}_i = 1.9 \times 10^5 \text{ photons/(mm}^2\text{)}$$

The spectral resolution of the VICS is limited by the resolution of the vidicon. As noted in Sections 2.4 and 2.5, the vidicon standard scan area ($A_v = 1.21 \text{ cm}^2$) is arbitrarily divided into 256 resolution elements on a side. Therefore, the pixel dimensions are

$$d_{vx} = 4.96 \times 10^{-2} \text{ mm}$$

and

$$d_{vy} = 3.72 \times 10^{-2} \text{ mm}$$

The spatial resolution of the VICS is

$$R_{\text{VICS}} (\text{spatial}) = \frac{d_{\text{vx}}}{M} \quad (11)$$

With a nominal $M = 0.6$,

$$R_{\text{VICS}} (\text{spatial}) = 82.7 \mu\text{m}.$$

The ideal spectral resolution of the VICS is then

$$R'_{\text{VICS}} (\text{spectral}) = R_{\text{VICS}} (\text{spatial}) (\text{RLD}) \quad (12)$$

in which RLD is identical to the reciprocal linear dispersion ($\text{\AA}/\text{mm}$) of the spectral device employed. However, in order to define a spectral feature, more than one pixel is necessary. On the basis of the percent definition of a feature as given in Ref. 1, four pixels are necessary to achieve 50-percent definition. Using this criterion, the realistic spectral resolution of the VICS is

$$R_{\text{VICS}} (\text{spectral}) = 4R'_{\text{VICS}} (\text{spectral}) \quad (13)$$

Therefore,

$$R_{\text{VICS}} (\text{spectral}) = (0.331 \text{ mm}) (\text{RLD}) \quad (14)$$

$R'_{\text{VICS}} (\text{spectral})$ was experimentally found to be 0.34\AA for a spectrometer with $\text{RLD} = 4.78 \text{\AA}/\text{mm}$, and this is within 15 percent of a calculated value of 0.4\AA . It is important to recognize, as noted in Ref. 1, that the resolution given by Eq. (14) may not be obtainable if the signal level is too low. Using relations given in Refs. 1 and 3 it has been calculated that for the VICS a photon input rate of $\leq 10^5$ photons/sec will decrease the resolution capability by an order of magnitude.

The electron gain curve of the intensifier (Fig. 5) was also checked by measuring signal level at various intensifier voltages and employing neutral density filters to prevent system saturation and permit measurement over the three order of magnitude range of the intensifier gain. The results are shown in Fig. 5 and are seen to follow the gain curve supplied by the manufacturer. The linearity of the system was also checked using a tungsten ribbon standard lamp and neutral density filters. The system count output as a function of relative light intensity is given in Fig. 24, and the excellent linearity of the system is observed.

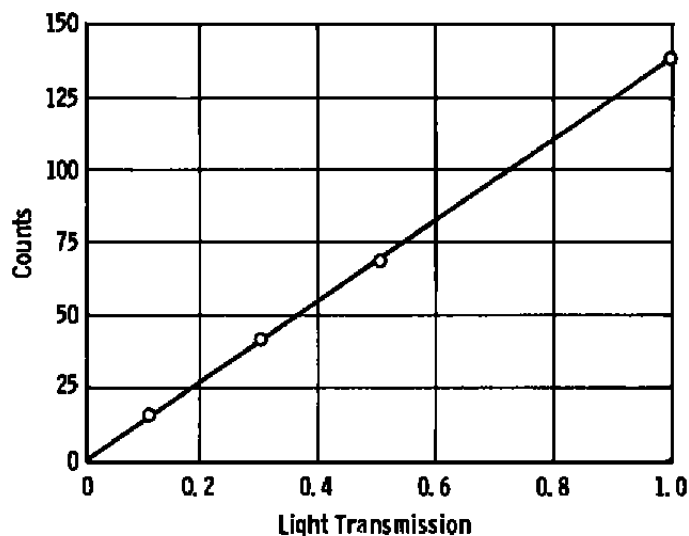


Figure 24. Linearity measurement of VICS.

4.2 MCPMT

With the MCPMT cooled to -50°C , the dark count rate per anode (pixel) is

$$n_{dl} = 1.1 \text{ photoelectrons/sec} \cdot \text{pixel}$$

Assuming a minimum counting time of 1 sec for continuous mode operation and a nominal q_e of 0.1, the minimum detectable exposure is

$$N_{ml} = 1.02 \times 10^3 \text{ photons/pixel} = 353 \text{ photons/mm}^2$$

For gated mode operation, the minimum detectable exposure is obviously

$$N_{ml} = 1 \times 10^3 \text{ photons/pixel} = 350 \text{ photons/mm}^2$$

The spatial resolution of the MCPMT is the dimension of the individual anodes, which are 1.7 mm by 1.7 mm. The ideal spectral resolution of the MCPMT is

$$R'_{\text{MCPMT (spectral)}} = 1.7 \text{ mm (RLD)} \quad (15)$$

Because of the large pixel size, the MCPMT would rarely be used for spectral scanning purposes; rather, it would be used for sampling specific portions of a known spectrum. The spectral range, as seen in Fig. 16, is limited to the 2000 to 8000 Å range, but this is quite sufficient for the flow diagnostic techniques at AEDC.

The output linearity of the MCPMT was checked for both the analog mode and photon-counting mode of operation, and as shown in Fig. 25 the linearity is within 5 percent over the four order of magnitude range of input light intensity. The relative gain of the MCPMT was measured as a function of applied voltage and is shown in Fig. 18 in comparison with nominal values from ITT. The absolute gain, G_e , was also measured at an applied voltage of 2580 volts, and the value is $G_e = 3.11 \times 10^6$, which is reasonable in comparison to the predicted maximum gain of 5×10^6 .

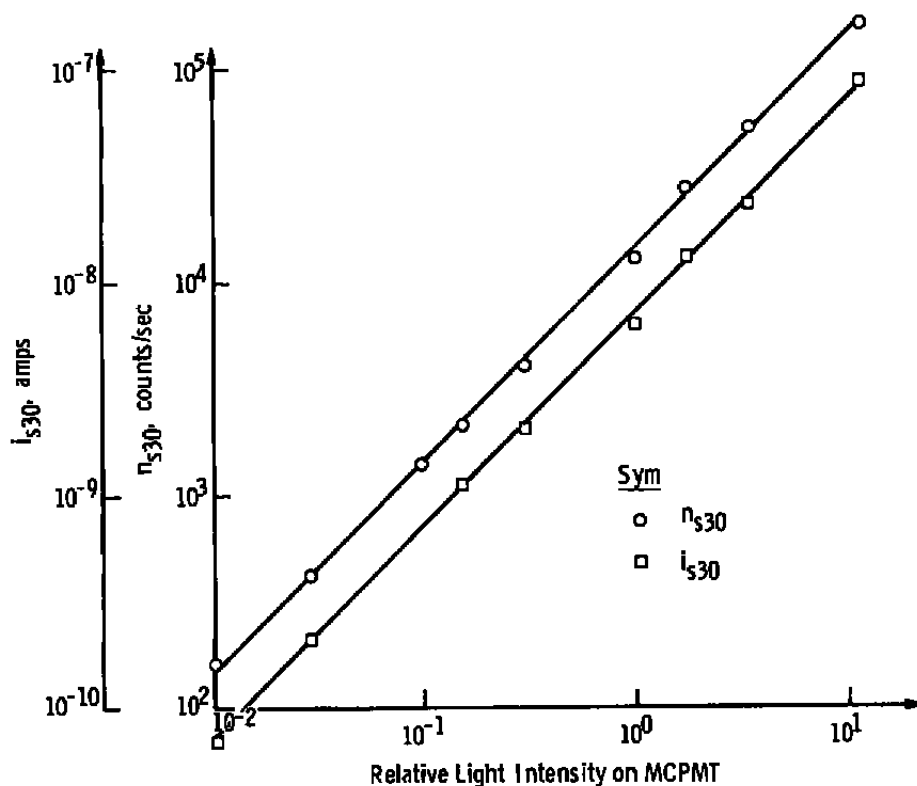


Figure 25. Linearity measurements of MCPMT.

Integral photoelectron count distribution curves for the MCPMT were obtained by measuring the count rates as a function of discriminator level setting, and a typical result is shown in Fig. 26 for uncooled tube operation. It is observed that the discriminator level setting that essentially rejects all low level electrical noise pulses gives a dark count rate equivalent to the measured dark current based on an MCPMT gain of 3.11×10^6 .

Photocathode uniformity was checked by using a spectrometer to provide a 50- μ m-wide image of the $\lambda = 546.1$ -nm mercury line on the MCPMT photocathode. By scanning the spectrometer the line image was subsequently swept across a group of 30 anodes coupled together (3 columns, 10 rows). Typical results of these scans are shown in Fig. 27, and they

indicate that the photocathode sensitivity will vary ± 5 percent across the surface. On the basis of the RLD of the spectrometer, the spectral coverage of the anode configuration could be calculated for comparison to the measured value, and as shown in Fig. 27, the two values could agree within 3 percent. Also noted in Fig. 27 is the excellent rectangular shape of the response curve which is most desirable for making intensity measurements of selected portions of spectra.

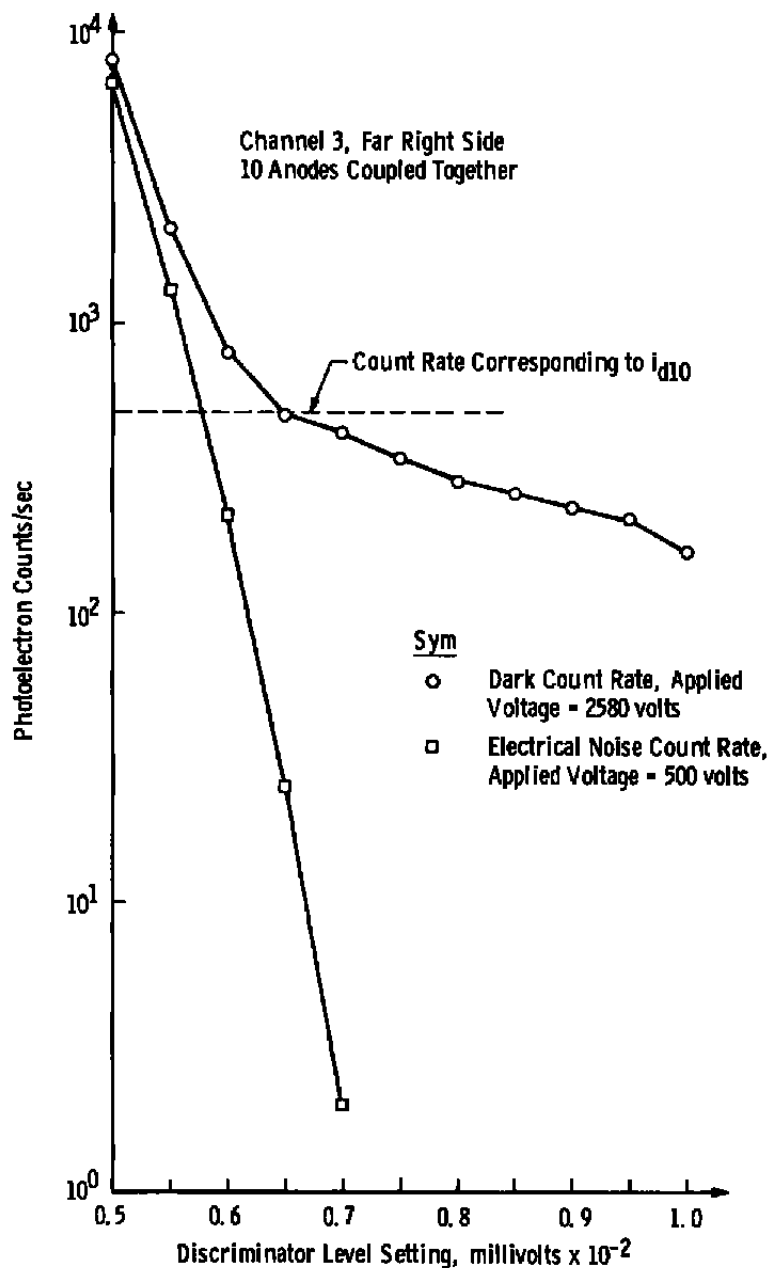


Figure 26. Integral photoelectron count distribution of MCPMT.

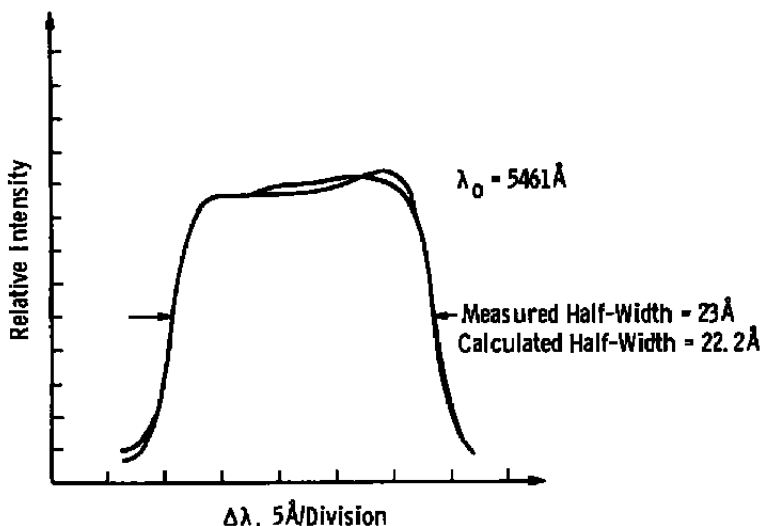


Figure 27. Wavelength scan profiles of two 30-anode groups of the MCPMT.

5.0 DISCUSSION

5.1 COMPARISON OF AEDC SYSTEMS AND A COMMERCIAL SYSTEM

The important characteristics of pixel size, spectral resolution and extent, and minimum required exposure are compared in Table 1 for the MCPMT, VICS, and the OMA-II® family of multichannel detection systems manufactured by EG&G (Ref. 5). In terms of required exposure based on photons/pixel, all these systems are comparable because they are essentially shot noise limited systems. However, for both high spectral/spatial resolution requirements, the VICS is the best system. If, on the other hand, spectral and spatial resolution can be sacrificed, the MCPMT has a sensitivity advantage of 2 to 3 orders of magnitude, and the MCPMT has the additional capability of being used in the photon counting mode over long counting times to achieve low imprecision. For making measurements over the widest possible spectral region the MCPMT and VICS have a decided advantage over the OMA-II. At present the most favorable characteristic of the OMA-II family is its wide variety of software, which offers very flexible data presentation and reduction methods.

5.2 METHODS FOR IMPROVEMENT OF AEDC SYSTEMS

Because the AEDC multichannel detection systems are in the shot noise regime, little can be done to improve their sensitivity for measurement of radiation in a continuous mode.

However, for pulsed mode radiation measurements the VICS and MCPMT can be improved with increased gain for greater single pulse precision. This can be achieved by using a three-stage intensifier with the VICS system for pulsed mode operation, increasing electron gain by approximately 100. Gain of the MCPMT system can be improved only by using preamplifiers at the anode outputs, and this is a necessity for using the MCPMT with the LeCroy gated integrator system when the pulsed radiation levels are low.

Table 1. Comparison of Multichannel Detection Systems

Type	OMA-2 (EG&G Model 1254E)	VICS 2-Stage Channel Intensifier (ITT) and Cooled Vidicon (GE)	MCPMT 3-Stage Channel Intensifier (ITT), 100 Anodes, Cooled
Pixel Size, mm ²	5.49×10^{-3}	1.85×10^{-3} (Vidicon) 5.29×10^{-4} (Intensifier)	2.89
Ideal Spectral Resolution, Å	RLD (7.44×10^{-2})	RLD (8.27×10^{-2})	RLD (1.7)
Spectral Extent, Å	RLD (12.2)	RLD (18.0)	RLD (18.0)
Equivalent Dark Rate Photon Input for 10 mm ² Spectral Image at 5000 Å, photons/sec	$\approx 9 \times 10^3$	$\approx 5 \times 10^3$	≈ 40
Minimum Required Exposure for SNR = 10	103 photons/pixel or 1.9×10^4 photons/mm ²	103 photons/pixel, or 1.9×10^5 photons/mm ²	1020 photons/pixel or 353 photons/mm ²
Maximum Integration Time	≈ 10 sec	2 min (Continuous Filament) 30 min (Gated Filament)	Limited Only by Experimental Requirements

Because of the glass input window of the VICS intensifier, the sensitivity of the system in the UV is greatly reduced (see Fig. 4). If a new intensifier can be obtained, it should be equipped with a UV fused silica window. However, in order to obtain immediate improvements of the VICS sensitivity in the UV spectral region, UV downconversion plates are being developed using sodium salicylate and coronene coatings (Ref. 6).

At present, the output capability of the MCPMT when mounted in its cooled housing is limited to 19 channels because of space limitations in the design of the cooler housing (see

Fig. 21). A new cooler housing must be designed to take advantage of the 100-channel capability of the MCPMT.

Perhaps the greatest and most easily obtainable improvement for the present AEDC systems will be the continued development of minicomputer software for increased flexibility in data acquisition and reduction. Of primary importance is the development of a capability for fitting of theoretical spectra or intensity ratios to similar measured quantities in a real time mode and for terminal display of both spatial and temporal variations of measured flow parameters.

As sampling rate requirements for nonperturbing flow diagnostic techniques reach the 100- to 1000-Hz level, the speed limitations of the present AEDC systems will be encountered. The MCPMT is limited to sampling rates of approximately 125 Hz because of the inherent dead time associated with microchannel plates (Ref. 7). The only method to raise this limit is through better design of microchannel plates. The VICS system is presently limited to single shot measurements at a rate of approximately 8.6 measurements per minute! This slowness is directly due to the inherent slowness of the floppy disk system used for storage as well as the slow speed of normal vidicon scanning. VICS data acquisition rates can be improved only with a frame grabber memory system and replacement of the vidicon with a charge injection device. These improvements for the VICS are presently being explored.

REFERENCES

1. Simon, R. E., ed. *RCA Electro-Optics Handbook*. Technical Series EOH-11, RCA Commercial Engineering, Harrison, New Jersey, 1974.
2. Eberhardt, E. H. "Image Intensifier Gain Nomograph." ITT Electron Tube Division, Fort Wayne, Indiana, 1972.
3. Eberhardt, E. H. "Resolution Specifications." ITT Research Memo No. 321, October 6, 1960.
4. Jones, J. H. "Software Techniques for Acquisition of Optical Data from a Mini-computer-Based Image-Intensifier-Vidicon System." AEDC-TR-79-43 (AD-A074844), September 1979.
5. "Advanced Multichannel Spectroscopy." EG&G Princeton Applied Research, 7416-20M-RP, February 1981.

6. Coleman, C. I. "Imaging Detectors for the Ultraviolet." *Applied Optics*, Vol. 20, No. 21, November 1, 1981, pp. 3693-3703.
7. Oba, Koichiro. *Microchannel Plate Photodetectors*. Hamamatsu TV Co., Ltd., Application RES-0792-01 (Second Edition).

NOMENCLATURE

A_v	Sensitive area of the vidicon for the standard scan, mm^2
ADC	Analog-to-digital converter
CTF	Contrast transfer function
c_e	Coupling efficiency of intensifier/vidicon coupling lens assembly
D	Vidicon diameter, mm
D/A	Digital-to-analog converter
d_i	Linear dimension of intensifier pixel, mm
d_{vx}, d_{vy}	Horizontal and vertical dimensions of vidicon pixel, respectively, mm
E, E', E''	Photon conversion efficiencies of intensifier phosphor; output photons/electron/ev of output photons, watts of radiation out/watts of electron energy dissipated in phosphor; number of photons out/number of electrons in, respectively
EBI	Intensifier equivalent brightness input, lumens/ cm^2
\bar{E}_p	Mean photon energy from the intensifier phosphor, ev
F_{20}	Relative luminous flux of P20 phosphor
G_B	Brightness gain of intensifier
G_p	Photon gain of intensifier

G, G_e	Relative and absolute electron gain of intensifier, respectively
I/O	Input/output
IC	Integrated circuit
i_{av}	Vidicon preamplifier equivalent dark photon input, rate = photons/sec • (pixel) _i
i_{di}	Dark current per anode of the MCPMT, amps
i_{di}	VICS equivalent dark photon input rate generated by the intensifier, photons/sec • (pixel) _i
i_{dv}	Vidicon thermally generated equivalent dark photon input rate, photons/sec • (pixel) _i
i_{mx1}	Maximum permissible average current for one anode of the MCPMT, amps
i_{s30}	Signal current of 30 anodes of the MCPMT, amps
i_{td}	Total dark current of the MCPMT, amps
LN ₂	Liquid nitrogen
ℓ_{pi}, ℓ_{pv}	Line pairs per millimeter for intensifier and vidicon, respectively
M	Magnification of the coupling optics between intensifier and vidicon
MCP	Microchannel plate
MCPMT	Multichannel photomultiplier tube
MIIVSS	Minicomputer-based image intensifier-vidicon system software
N_{di}	VICS equivalent dark photon input generated by the intensifier, photons/(pixel) _i

N_{dv}	Vidicon-generated equivalent dark photon input, photons/(pixel) _i
N_{dvics}	VKS total equivalent dark photon input, photons/(pixel) _i
N_{m1}	Minimum detectable exposure of MCPMT, photons/pixel
N_s, N_{smin}	Detector input signal and minimum acceptable exposure, photons/pixel
n_{d1}	Dark count rate per pixel (anode) of the MCPMT, photoelectron counts/sec • pixel
n_{s30}	Signal count rate for 30 pixels (anodes) of the MCPMT, photoelectron counts/sec
n_{td}	Total dark count rate of the MCPMT, photoelectron counts/sec
PMT	Photomultiplier tube
pixel	Picture element
q_e	Quantum efficiency
R_{ia}	Absolute spectral response of the intensifier, amps/watt
$R'_{MCPMT(spectral)}$	Ideal spectral resolution of the MCPMT
RLD	Reciprocal linear dispersion of the spectral device connected to one of the multichannel detection systems, Å/mm
R_{TV}, R'_{TV}	Vidicon resolution in TV lines per raster height and per raster diagonal, respectively
R_{va}	Absolute spectral response of the vidicon, amps/watt
R_{VFS}	Full spectrum response of vidicon
$R_{VICS(spatial)}$	Spatial resolution of VICS
$R'_{VICS(spectral)}, R_{VICS(spectral)}$	Ideal and realistic spectral resolution of VICS, respectively, Å

SNR	Signal-to-noise ratio
V	Effective accelerating voltage of intensifier, ev
V_p	Mean energy of electrons striking intensifier phosphor, ev
VICS	Vidicon/intensifier coupled system
N_{cf}	Mean transmittance of the coupling optics lens system for VICS
λ	Wavelength, Å or nm
τ_{gi}	Intensifier gate interval, sec
τ_{ov}	Vidicon exposure time, sec
τ_{px}	Pixel readout time, sec
Φ_i	Intensifier luminous sensitivity, μ amps/lumen
Ω_{cf}	Collection solid angle of coupling optics of VICS